1

Introduction

1.1 Characterization of Hydrocarbon Reservoirs

Hydrocarbon accumulation requires the presence of a natural trap consisting of reservoir rocks, sealing or caprocks, and three-dimensional four-way closure. The description of reservoir rocks should include the following elements:

1. Presence of reservoir rocks
   - Depositional model (sequence stratigraphy framework)
   - Lithology
   - Structural characteristics
   - Lateral and vertical distribution
2. Quality of reservoir rocks
   - Lateral continuity and extension
   - Thickness and vertical lithological cyclicity
   - Relative heterogeneity of rock properties
   - Pore systems ranges and types
   - Transmissibility of fluids
   - Hydrocarbon potential and preservation
   - Diagenetic characteristics

The reservoir rocks are mainly sedimentary rocks, which are deposited as sediments by water, wind, or ice and made up of clastic material, chemical precipitates, and organic or biogenic debris. Sedimentary rocks have formed from sediments or debris by any of the following processes: (1) *compaction*, (2) *cementation*, and (3) *crystallization*. A simplified classification of sedimentary rocks is presented in Table 1.1.

Clastic rocks are the consolidated sedimentary rocks consisting principally of the debris of preexisting rocks (of any origin) or the solid products formed during chemical weathering of such rocks, transported mechanically (by such agents as water, wind, ice, and

Leonid Buryakovsky, George V. Chilingar, Herman H. Rieke and Sanghee Shin
Petrophysics, (1–56) © Scrivener Publishing LLC

Table 1.1 Simplified classification of sedimentary rocks.

Clastic Rocks	Carbonates	Evaporites	Organic Rocks	Other
Conglomerate	Limestone	Gypsum	Peat	Chert
Breccia	Chalk	Anhydrite	Coal	
Sandstone	Dolomite	Rock salt	Diatomite	
Siltstone	Marl	Potash	Limestone	
Mudstone				
Shale				
Limestone				

gravity) to their places of deposition. Clastic non-carbonate rocks, which are almost exclusively silicon-bearing (either as quartz or silicates) are called the *siliciclastic rocks*. Siliciclastic rocks consist of sand-, silt- and clay-size particles and their combinations.

Carbonate rocks are the rocks consisting chiefly of carbonate minerals formed by the organic or inorganic precipitation from aqueous solution of carbonates of calcium (limestone), calcium plus magnesium (dolomite), or iron (siderite). These rocks may consist also of the debris of preexisting carbonate rocks (of any origin), which have been transported mechanically to their places of deposition.

Chilingar and Yen (1982) pointed out that carbonate rocks constitute only 15 to 30% of the total volume of sedimentary rocks, whereas about 65% of the total oil and gas reserves in the World reside in carbonate reservoirs. The behavior of carbonate reservoirs differs in many respects from sandstone reservoir, mainly due to the very complex pore structure of carbonate rocks. However, the percentage of in-situ oil recovered from these reservoir rocks is often very low ($\leq 20\%$). Their origin, composition, and the diagenetic and catagenetic processes in large measure determine the petrophysical properties of carbonates and behavior of carbonate hydrocarbon reservoirs (refer to Chilingarian *et al.*, 1996).

Chert is a hard, extremely dense or compact cryptocrystalline sedimentary rock, consisting dominantly of cryptocrystalline silica (chiefly fibrous chalcedony) with lesser amount of micro- or cryptocrystalline quartz and amorphous silica (opal).

Figure 1.1 illustrates a classification based on a tetrahedron at the corners of which are placed carbonate, clay (shale), sandstone (quartz) and chert. This figure also depicts one side of this

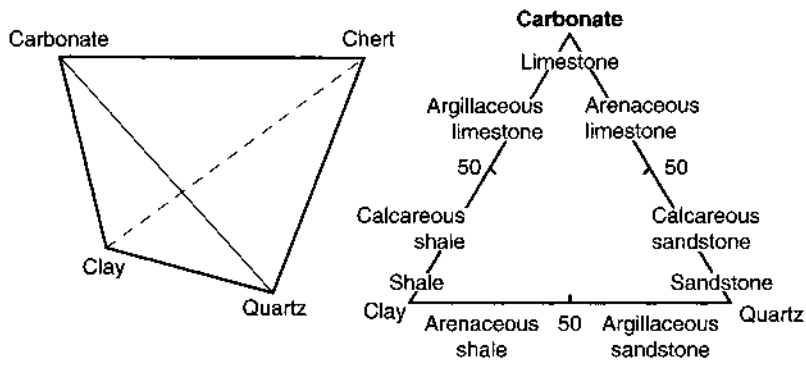

Figure 1.1 Fundamental tetrahedron for classifying sedimentary rocks.

tetrahedron so that some of the variations between contents of shale, sandstone and limestone can be seen. For example, starting from shale and going toward limestone, increasing amounts of lime will produce calcareous shale, grading into argillaceous (shaley) limestone, then to pure limestone. Similarly, on the other two edges, it is shown how the changes occur from shale to sandstone and from sandstone to limestone. The other three sides show similar variations with chert replacing one of the other constituents. Other valuable classifications of sandstones based on composition were presented by Teodorovich (1965). (e.g., Figure 1.2a,b.)

One of the most important aspects in reservoir characterization is an understanding of depositional environments in the area under study. Depositional environments and facies relationships, diagenesis (physical and chemical changes in sediments up to and *through*

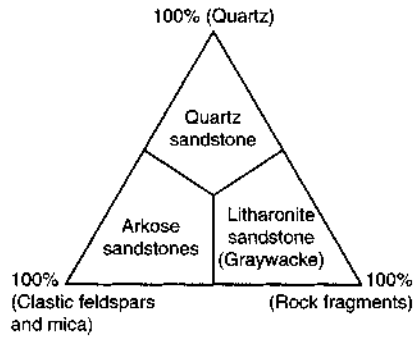

Figure 1.2a The major classification of sandstones, based on composition. (After Teodorovich, 1965.)

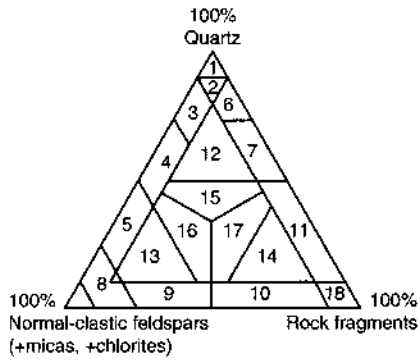

Figure 1.2b Classification of sandstones on the basis of mineralogical composition. (A) Family of quartz sandstones (1, 2, 3); (B) arkoses (4, 5); (C) two-component mineral-petroclastic sandstones (6, 7, 8, 9, 10, 11) – the latter family can be subdivided into (a) predominantly quartz sandstones (6, 7); (b) predominantly feldspathic sandstones (8, 9), and (c) predominantly petroclastic sandstones (10, 11): (D) three-component mineral – petroclastic sandstones with absolute predominance of one of the components (12, 13, 14); (E) three-component mineral – petroclastic sandstones with relative predominance of one of the components (15, 16, 17); (F) ultrapetroclastic sandstones (18). (After Teodorovich, 1967, Figure 1, p. 76.)

lithification) and catagenesis (physical and chemical changes in the lithified rock) strongly affect the size, shape, pore-space geometry, porosity, permeability, and location of clastic deposits.

Any sediment has originally a terrestrial *source* (place of origin), created by the life cycles of plants or animals (e.g., shells, leaves, logs, and organic sediments), or by weathering (chemical disintegration and physical breakdown) of parent rocks. Each sediment has a *provenance*, which is the particular area from which its components were derived and transported by water, ice, or wind into the place of *deposition*. Sediments are deposited under a variety of conditions or environments, both on land and at sea. Each environment is characterized by specific physical processes and has the particular plants and animals living within it, which contribute such fossils as bones, shells, and plant fragments. Simplified classification of environments of sediment deposition is shown in Table 1.2.

As an example, the depositional environment and stratigraphy of the South Caspian Basin are presented here owing to the geological complexity of the basin and familiarity by the authors with the area.

Table 1.2 Depositional environments.

<table>
<tr><th></th><th colspan="2">Delta Group</th><th colspan="2">Intradelta Group</th></tr>
<tr><td rowspan="2">Continental</td><td colspan="2">Aeolian deposits</td><td colspan="2">Aeolian deposits</td></tr>
<tr><td colspan="2">Alluvial deposits</td><td colspan="2" rowspan="2">Alluvial deposits</td></tr>
<tr><td rowspan="2">Transitional</td><td rowspan="3">Deltaic deposits</td><td>Delta-plain deposits</td></tr>
<tr><td rowspan="2">Prodelta-plain deposits</td><td colspan="2" rowspan="2">Coastal Intradelta-marine deposits</td></tr>
<tr><td rowspan="3">Marine</td><td rowspan="3">Normal marine deposits</td><td rowspan="3">Normal marine deposits</td><td>Shelf deposits</td></tr>
<tr><td>Slope deposits</td><td>Slope deposits</td></tr>
<tr><td>Deep marine deposits</td><td>Deep marine deposits</td></tr>
</table>

1.1.1 Geographical and Geological Background of the South Caspian Basin

The South Caspian Basin encompasses water areas of the South Caspian Sea, and together with land areas of Eastern Azerbaijan and Western Turkmenistan constitutes the southern portion of the Caspian Sea region (Figure 1.3a). The South Caspian Basin is separated from the Middle Caspian Basin by the Absheron-Prebalkhan zone of uplifts, which extends NW-SE connecting the Absheron and Cheleken peninsulas, forming a narrow submarine ridge (Buryakovsky, 1974c, 1993a, 1993b; Buryakovsky *et al.*, 2001) (Figures 1.3b and 1.3c).

Azerbaijan borders Russia to the north, Georgia and Armenia to the west, Turkey and Iran to the south, and the Caspian Sea to the east. Aerially, it encompasses the southeastern spurs of the

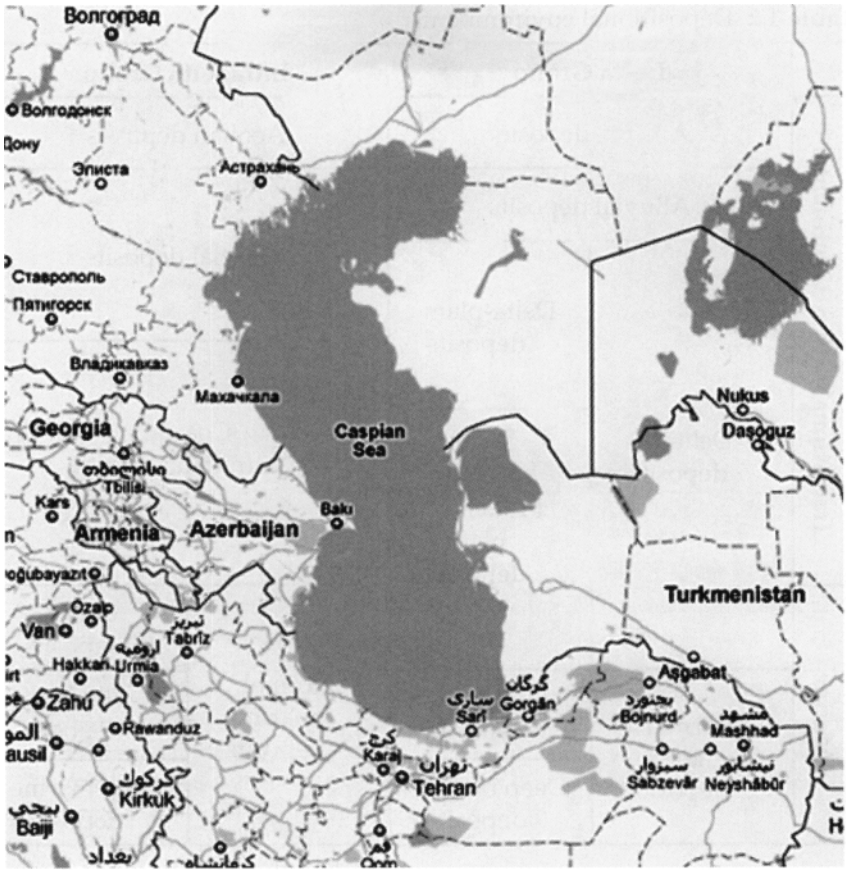

Figure 1.3a Caspian Sea Region. (Modified after National Geographic Society Map, Washington, D.C., 1999.)

Greater and Lesser Caucasus Mountains, the Kura Intermountain Depression, and Talysh Mountains (Figure 1.4 and 1.5). Azerbaijan is one of the oldest oil and gas provinces in the world. For more than 140 years oil and gas has been commercially produced onshore in Azerbaijan. The offshore production at the Caspian Sea began about 100 years ago.

Turkmenistan borders Kazakhstan to the north, Uzbekistan to the northeast and east, Afghanistan and Iran to the south, and the South Caspian Sea to the west. The onshore portion of Western Turkmenistan includes the Cheleken Peninsula on the northwest and is bordered by the Kopet-Dagh Mountains to the south.

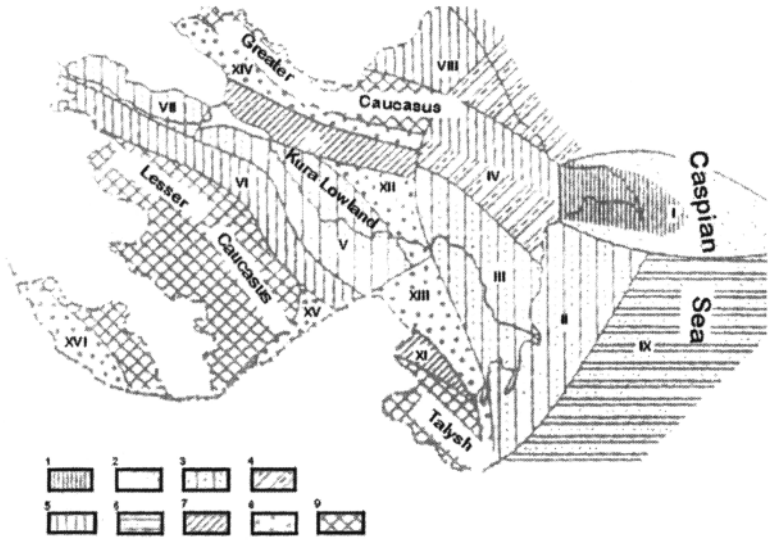

Figure 1.3b Oil and gas regional distribution, and fields and prospects of Azerbaijan and the South Caspian Basin. (Modified after the Excursion Guide-Book for Azerbaijan SSR, Vol. 1, 1984.) 1–Boundaries between oil- and gas-bearing regions, 2–boundaries between oil- and gas-bearing areas, 3–oil fields, 4–gas and gas-condensate fields; oil- and gas-bearing areas: 5–high oil and gas content, 6–moderate oil and gas content, 7–potential structure, 8–structure with low potential. Oil and gas-bearing regions and areas (areas are shown in circles): 1–Apsheron-Gobustan region (areas: 1–Aspheron; 2–Shemakha-Gobustan); II–Pre-Caspian-Kuba region; III–Kura region (areas: 3–Lower Kura, 4–Kyurdamir, 5–Gyandzha, 6–Adzhinour, 7–Kura-lori interfluve, 8–Alazan-Agrichai, 9–Dzhalilabad, 10–Baku Archipelago); IV–Araks area. Fields: 1–Balakhany-Sabunchi-Ramany, 2–Surakhany, 3–Karachukhur-Zykh, 4–Gum Deniz, 5–Goudsny, 6–Kala, 7–Buzovny-Mashtagi, 8–Darvin Bank, 9–Pirallaghi Adasi, 10–Gyurgyan Deniz, 11–Chalov Adasi, 12–Azi Aslanov, 13–Palchygh Pilpilasi-Neft Dashlary, 14–Dzanub, 15–Bakhar, 16–Binagady-Chakhnaglyar, 17–Sulutepe, 18–Yasamaly Valley, 19–Bibielbat, 20–Puta-Lokbatan, 21–Kyorgyoz-Kzyltepe, 22–Karadag, 23–Shongar, 24–Umbaki, 25–Duvanny, 26–Dashgil, 27–Chondagar-Zorat, 28–Siazan-Nardaran, 29–Saadan, 30–Amirkhanly, 31–Eastern Zagly, 32–Zagly-Tengialty, 33–Kyurovdag, 34–Karabagly, 35–Khillin, 36–Neftechala, 37–Kyursangya, 38–Mishovdag, 39–Kalmas, 40–Pirsagat, 41–Malyl Kharami, 42–Kalamadyn, 43–Muradkanly, 44–Kazanbulag, 45–Adzhidere, 46–Naftalan, 47–Mirbashir, 48–Sangachal, 49–Duvanny Deniz, 50–Khara Zyrya, 51–Bulla Deniz, and 52–Garasu.

The offshore region includes the eastern portion of the Absheron-Prebalkhan anticlinal trend and the Chikishlyar-Okarem zone (Turkmenian structural terrace); to the south it is bordered by the Alborz Range in Iran.

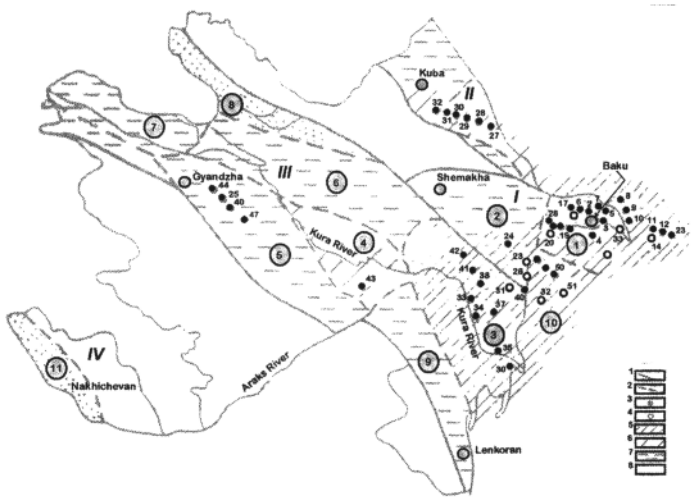

Figure 1.3c Regional distribution of oil and gas in Azerbaijan and the South Caspian Basin. (Modified after Aliyev *et al.*, 1985.) Regions: 1–with significant, proved, initial potential resources; 2–highly favorable (offshore); categories of favorability: 3–first, 4–second, 5–third; 6–areas favorable for oil and gas; 7–areas possibly favorable; 8–areas with unclarified prospects; 9–areas with no prospects. Oil- and gas-bearing areas; I–Apsheron, II–Baku Archipelago, III–Lower Kura, IV–Schemakha-Gobustan; V–Yevlakh-Agdzhabedy; VI–Gyandzha, VII–Kura-lori interfluve, VIII–Pre-Caspian-Kuba, IX–deep-water parts of the South Caspian Basin probably favorable areas: X–Adzhinour, XI–Dzhalilabad; areas with uncertain potential: XII–Dzharly-Saatly, XIII–Mil-Mugan, XIV–Alazan-Agrichai, XV–Araks, and XVI–Nakhichevan.

There are several oil and gas regions within onshore Azerbaijan. The main regions are (from north to south):

1. Pre-Caspian – Kuba Region
2. Absheron Peninsula
3. Kobystan anticlinal belt
4. Kura Intermountain Depression.

There are four offshore oil and gas regions that are within the Azerbaijan sector of the Caspian Sea (from north to south):

1. Absheron Archipelago
2. Western portion of the Absheron-Prebalkhan zone of uplifts
3. South Absheron offshore zone
4. Baku Archipelago.

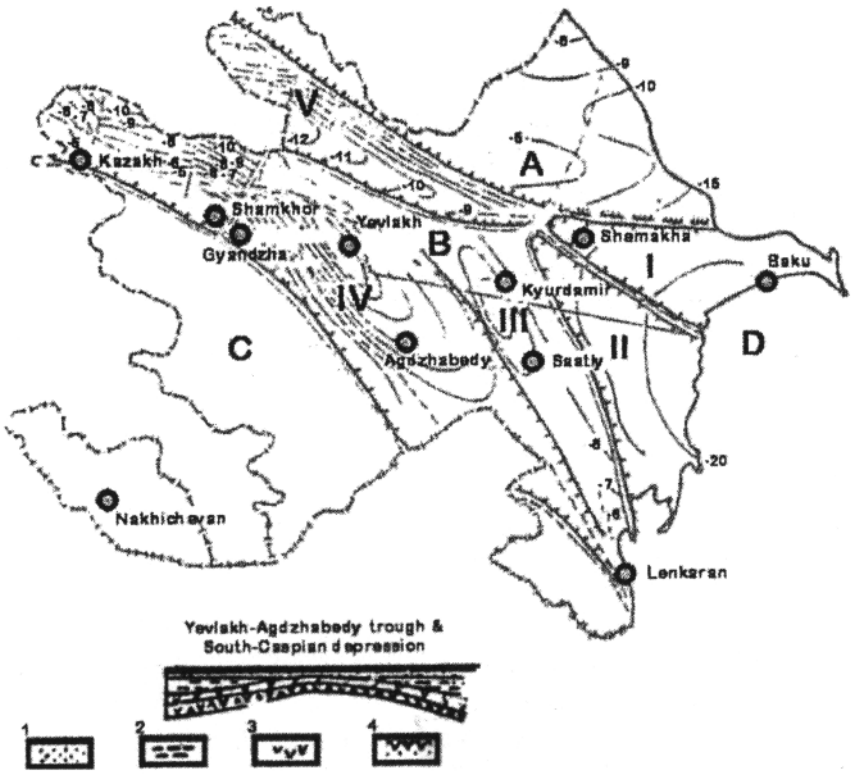

Figure 1.4 Structural pattern of Azerbaijan. (Modified after the Excursion Guide Book for Azerbaijan SSR, Vol. 11, 1984.) A–Greater Caucasus Anticlinorium; B–Kura Intermontane Depression; C–Lesser Caucasus Anticlinorium; D–South Caspian Basin: I–Gobustan-Apsheron Trough; II–Lower Kura Trough; III–Geokchai-Saatly Anticlinal Trend; IV–Yevlakh-Agdzhabedy Trough; V–Lori-Adzhinour Trough. 1–Quaternary, 2–Miocene-Paleogene, 3–Mesozoic, and 4–consolidated crust.

Offshore fields are located over the plunges of the Absheron Peninsula and the southeast Kobystan anticlinal belt.

1.1.2 Sedimentary Features of Productive Horizons in the South Caspian Basin

The main Middle Pliocene productive unit in Azerbaijan and the South Caspian Basin is called the Productive Series (sand, silt and shale interbedding). Sand-silt reservoirs contain argillaceous

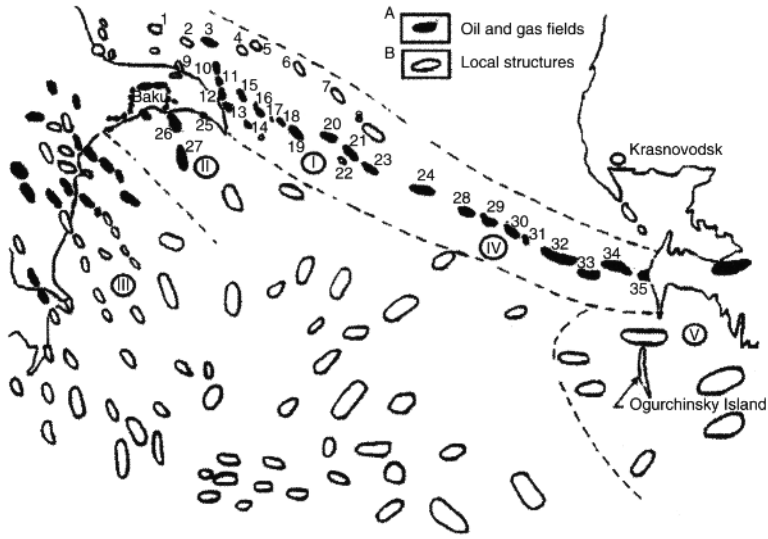

Figure 1.5 Location of structures on the Absheron Threshold. (Modified after Bagir-zadeh *et al.*, 1974.) A–Oil and gas fields; B–prospects: 1–Goshadash, 2–Apsheron Bank, 3–Agburun Deniz, 4–Gilavar, 5–East Gilavar, 6–Danulduzu, 7–Ashrafi, 8–Agburun, 9–Mardakyan Deniz, 10–Darvin Bank, 11–Pirallaghi Adasi (Northern Fold), 12–Pirallaghi Adasi (Southern Fold), 13–Gyurgyan Deniz, 14–Dzhanub, 15–Khali, 16–Chalov Adasi, 17–Azi Aslanov, 18–Palchygh Pilpilasi, 19–Neft Dashlary, 20–Gyuneshli, 21–Chyragh, 22–Ushakov, 23–Azeri, 24–Kyapaz, 25–Shakh Deniz, 26–Gum Deniz, 27–Bakhar, 28–Livanov-West, 29–Livanov-Center, 30 Livanov-East, 31– Barinov, 32–Gubkin (Western, Central, Eastern), 33–Zhdanov (Western, Eastern, Pre-Cheleken Dome), 34–LAM, 35–Cheleken.

material, whereas the shale contains sand and silt components. Stratigraphic section and typical well logs (resistivity and SP) of the Productive Series, Azerbaijan, are given in Figure 1.6 and 1.7. The thickness of the Productive Series increases in the direction of the central part of the South Caspian Basin from 1500 m within the Absheron Peninsula to 3150 m within the Absheron Archipelago, to 4150 m within the South Absheron Offshore Zone, and to 4400 m within the Baku Archipelago.

The Productive Series includes the following formations:

1. Upper division
   a. Surakhany
   b. Sabunchi
   c. Balakhany
   d. Fasila

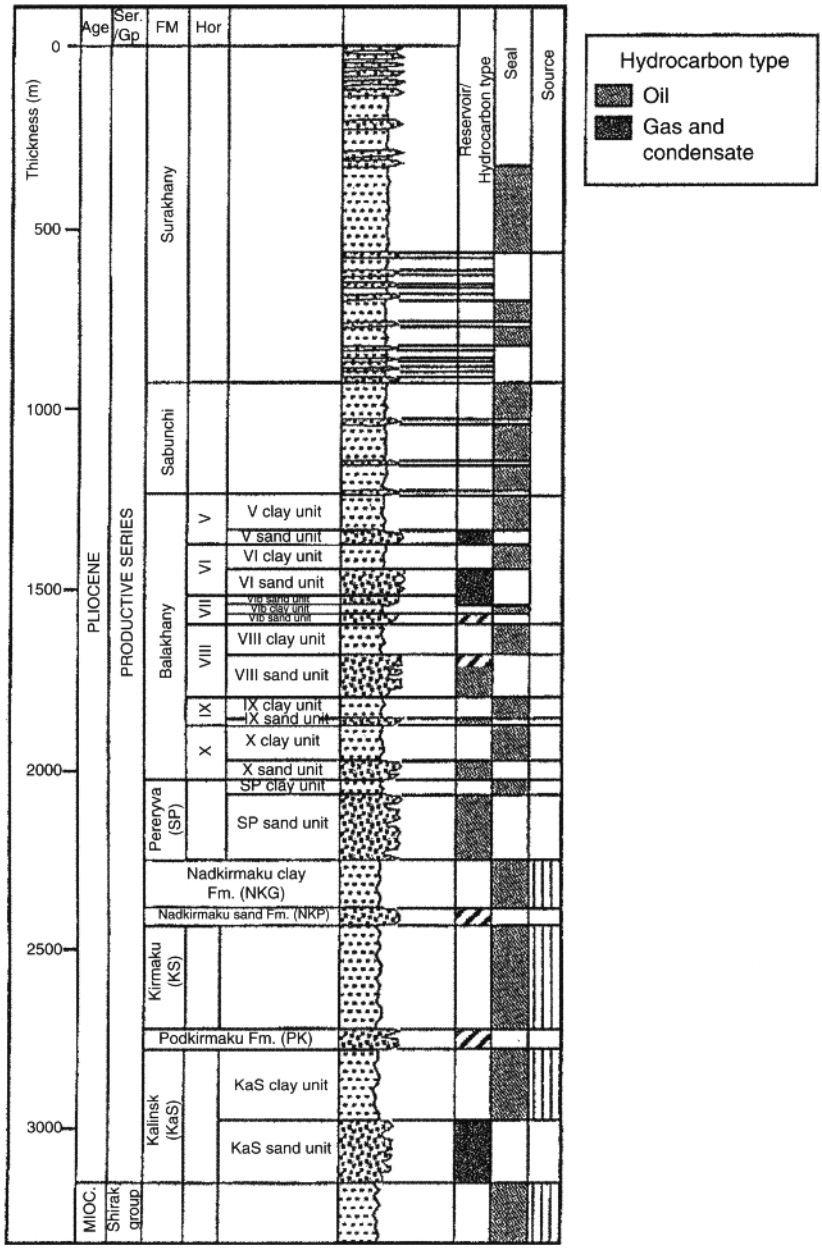

Figure 1.6 Productive series stratigraphic/lithologic column.

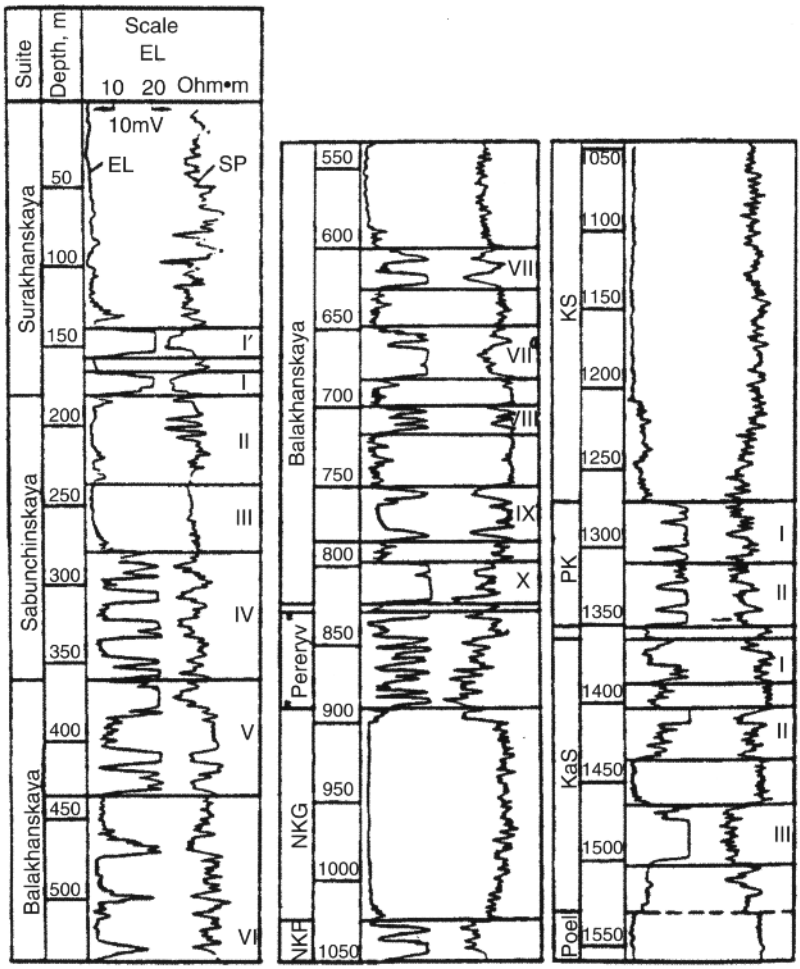

Figure 1.7 Typical resistivity logs of the productive series.

2. Lower division
   a. Nadkirmaku Shale
   b. Nadkirmaku Sand
   c. Kirmaku
   d. Podkirmaku
   e. Kala

The terrigenous (siliciclastic) rocks of Productive Series have gray color in the lower division, whereas above they are grayish brown. The rocks within the Absheron Peninsula are composed of

quartz and feldspar, whereas within the Absheron and Baku archipelagoes they become polimictic-arkose, arkosic-graywacke and graywacke. The cement is usually composed of clay and calcite with a significant predominance of clay. Sorting of the siliciclastics improves noticeably upward in each sedimentary sequence.

1.1.3 Depositional Environment of Productive Series, Azerbaijan

Core data, paleontological and log analyses suggest that the Productive Series sediments were deposited in a relatively shallow-water, fluvial-deltaic environment as is evident from the paleogeographic and subsidence curves (Figure 1.8). The large volume of clastic rocks, forming the Productive Series, indicates the proximity of sediment sources. The Russian Platform, Kilyazi-Krasnovodsk anticlinal trend, islands existing north of the Absheron Peninsula and Absheron Archipelago, and the southeastern slope of the Greater Caucasus, served as primary sources for clastic material (Absheron type lithofacies) for Absheron Peninsula and the adjacent Caspian Sea offshore. Weathering of older Mesozoic-Paleogene volcanic and

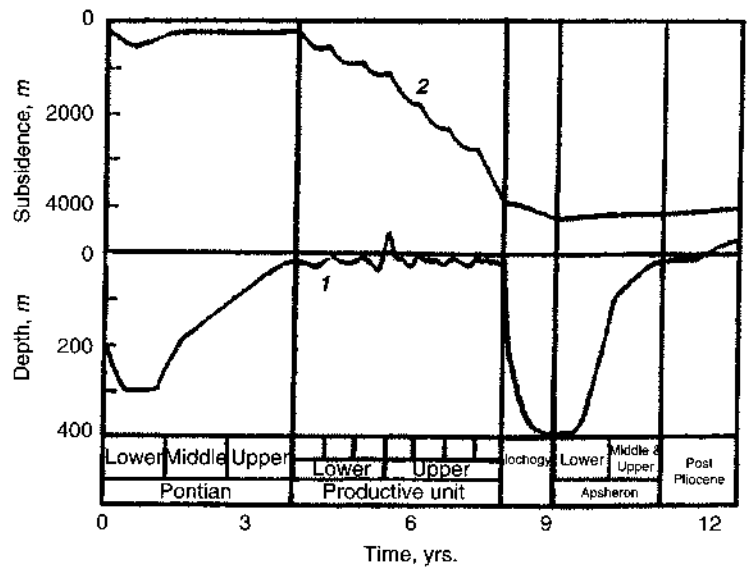

Figure 1.8 Pliocene paleogeographic (paleodepth) curve (1) and subsidence curve (2) for the Absheron Peninsula and adjacent offshore areas. (Modified after Buryakovsky *et al.*, 1982.)

sedimentary rocks from the Greater and Lesser Caucasus and Talysh Mountains, served as primary sources (Gobustan type of lithofacies) of sediments for the Lower Kura Region and the Baku Archipelago. The clastics were transported and deposited by Paleo-Volga, Paleo-Ural, Paleo-Kura and other paleo-rivers.

The major distribution pattern for reservoir rocks in the Absheron Oil and Gas Region as a whole, and within individual areas in particular, is a systematic change in mineral composition and decrease in grain size with increasing distance from the provenance (Buryakovsky, 1970, 1974c). With increasing distance to the south and southeast from the paleo-shoreline of the North Caspian Sea, depth to the productive reservoirs increases, sand content decreases, and shale and silt contents increase. More drastic changes occur in the transitional zone from the Absheron Peninsula, Absheron Archipelago and South Absheron Offshore Zone to the northern Baku Archipelago, where Absheron-type lithofacies, although preserving their main features, include more Gobustan-type lithofacies. The main changes are the following:

a. Shale content increases from 15% to 40%.
b. Sand content decreases from 40% to 15%.
c. Silt content changes in the range of 40% to 62%.
d. Grain size decreases from 0.08 to 0.02 mm.
e. Sorting is practically constant.

The Productive Series is divided into seven sedimentary sequences according to the transgressive/regressive cycles during development of the sedimentary basin. Upward through the section, they are:

1. Kala Formation (KaS)
2. Podkirmaku and Kirmaku formations (PK + KS)
3. Nadkirmaku Sand and Nadkirmaku Shale formations (NKP + NKG)
4. Fasila Formation plus X and IX Balakhany units
5. VIII, VII and VI Balakhany units
6. V Balakhany unit and IV, III and II Sabunchi units
7. I, I', A, B, C, D Surakhany units.

Each sequence displays fining upward, from coarse-grained sands at the base to the finer sands, siltstones and shales at the top. Furthermore, in each sequence, the shale content increases

and the sand content decreases up the stratigraphic column. For instance, within the fifth sequence at the Bakhar Field, shale content increases upward from 17.8% in Unit VIII to 29.9% in Unit VI; silt content changes, respectively, from 49.2% to 69.1%, and sand content decreases from 33.0 to 2.0%. This depositional pattern is dependent on the tectonic regime and depositional environment of the South Caspian Basin.

Shallow-marine fossils, fresh-water ostracods, and glauconite in the core samples indicate a mingling of marine and continental environments, especially at the base of each transgressive/regressive cycle. Individual layers in the suites of the Productive Series have been identified as stream-mouth bar deposits, distributary channel-fill sands, point-bar sands, crevasse sands, or transgressive-sheet deposits. Stream-mouth bar and point-bar deposits often occur as a deltaic couplet with point-bar sands of the delta plain prograding across underlying stream-mouth bars of the delta front. These delta-plain deposits either cut into or are slightly separated from the underlying delta-front deposits. Such a deltaic couplet is often found throughout the Absheron Peninsula and Absheron Archipelago at the base of Fasila Suite (the first break in deposition). More distinct rocks, however, characterize the upper intervals of each transgressive/regressive cycle. This portion of upper parts of transgressive/regressive cycles appears to indicate the migration of delta or distributary-channel system, such that the delta began to build elsewhere. Many of these rocks appear to be crevasse sands formed as the distributary reached the flood stage and broke through a levee into adjacent interdistributary bay areas.

Due to increase in shale content upward for each cycle throughout the stratigraphic section, the reservoir thickness diminishes to the upper part of each cycle and clearly affects log responses (for example, average resistivity decreases toward the top of each cycle). Principles of cyclic sedimentation were applied for subdividing the sedimentary section and for selecting intervals for reserve estimation.

To analyze the sequences of the Productive Series sedimentary section, the authors used a special parameter, which demonstrates relative sand content within an individual transgressive/regressive cycle. The individual cycle consists of two layers, i.e., sand/silt (reservoir rock) and shale (non-reservoir rock). Ratios of sand-silt to shale layers within each individual transgressive/regressive cycle allow plotting the curve of sand content variation in the entire sedimentary sequence. When the individual cycles are combined to constitute a

sequence of higher order, there is an overall decrease in the sand, and the shale content increases toward the sequence top. On this basis, the authors have defined the following levels of cyclic sequences:

1. Unit (with two layers).
2. Pack (with 4 to 6 layers).
3. Group (with 8 to 12 layers).
4. Formation (with 12 to 30 layers or more).

Individual layers can be defined as the group of layers where one observes a large increase in the shale content toward the sequence top. This provides a systematic correlation within the area and indicates the oil and gas contents. The formation level applies to thick sequences (suites), which have been identified at the Absheron Peninsula by a number of scientists on the basis of grain-size distribution and mineral composition of sedimentary rocks (Potapov, 1954, 1964). This procedure is used for well log stratigraphic correlations.

1.2 Reservoir Lithologies

The most common reservoir rocks are sands, sandstones, and carbonates including limestone and dolomite (Pustovalov, 1940; Pettijohn, 1957). Sometimes the weathered and fractured igneous and volcanic rocks may serve as the oil and gas reservoirs. To be commercially productive, the reservoir rocks must have sufficient thickness, areal extent, and pore space to contain an appreciable volume of hydrocarbons, and must yield the contained fluids at a satisfactory rate when the reservoir is penetrated by a well.

1.2.1 Clastic Rocks

Clastic rocks (mainly siliciclastics) are the good reservoir rocks, which are made-up from granular rocks, such as sands, sandstones, siltstones and sand-silt varieties. The key characteristics of clastic rocks are: (1) grain-size distribution, (2) grain sorting and rounding, (3) cement type and distribution, (4) structure and texture of a rock, (5) geometry of pore space and grain packing system, and (6) porosity and permeability.

1.2.1.1 Grain-size Characteristics of Clastic Rocks

The granular rocks are characterized by the *grain* or *particle size*, which ranges from colloidal particles up to pebbles and boulders.

Other characteristics of grains are their *sorting* and *roundness*. Poorly sorted sediments are composed of many different sizes and/or densities of grains mixed together. Well-sorted sediments, however, are composed of grains that are of similar size and/or density. Well-sorted sediments are usually composed of well-rounded grains, because the grains have been abraded and rounded during transportation. Conversely, poorly sorted sediments are usually angular, because of the lack of abrasion during transportation. The sharpness of corners on grains of sediment, viewed in profile (side view), is a measure of roundness. The well-rounded, subrounded, subangular, and angular grains are distinguished.

To understand grain-size distribution, as well as sorting and roundness of grains in a given rock, a grain-size analysis is applied along with the following procedures.

1. Direct measurement and observation of individual fragments of pebbles, cobbles, and bounders.
2. Sieving to separate pebbles, sand, and coarse silt.
3. Settling velocity for measuring the size of silt and clay particles.
4. Microscopic observation of sand, silt, and clay particles.
5. Scanning electron microscopy for studying of very small sedimentary features.

The smaller particles are defined by their volumetric diameters, i.e., the diameter of a sphere with the sane volume as the particle. The statistical proportions or distribution of particles of defined size fraction of sediment or rock is determined from the particle-size analysis.

There are numerous grain-size classifications. Examples include: Udden grade scale, Wentworth grade scale, Atterberg grade scale, Tyler standard grade scale, and Alling grade scale. Each of these scales is logarithmic. In American practices, the grain size is measured by the logarithmic grade scale devised by Udden in 1898 (Udden, 1914). This scale uses 1 mm as the reference point and progresses by the fixed ratio of ½ in the direction of decreasing size and of 2 in the direction of increasing size, such as 0.25, 0.5, 1, 2, 4. The extended version of the Udden grade scale was proposed by Wentworth (1922, 1924), who modified the size limits for the common grade terms, but retained the geometric interval or constant ratio of ½. The scale ranges from clay particles (diameter less

than 1/256 mm) to boulders (diameter greater than 256 mm). The Wentworth grade scale was modified by Krumbein in 1934, who proposed a logarithmic transformation of the scale, in which the negative logarithm to the base 2 of the particle diameter (in millimeters) is substituted for the diameter value, i.e., $\varphi = -\log_2 d$, where φ is the phi value and d is the particle diameter. The integers for the class limit range from –5 for 32 mm to +10 for 1/1024 mm (refer to Table 1.3). The classification of the grain size of sedimentary rocks is shown in Table 1.4 and Table 1.5.

Table 1.3 Pore/grain size diameter conversion table (millimeter to phi units).

mm	ϕ
4.00	–2.00
3.36	–1.75
2.83	–1.50
2.38	–1.25
2.00	–1.00
1.68	–0.75
1.41	–0.50
1.19	–0.25
1.00	0.00
0.841	0.25
0.707	0.50
0.500	1.00
0.420	1.25
0.351	1.50
0.297	1.75
0.250	2.00
0.210	2.25
0.177	2.50
0.149	2.75
0.125	3.00
0.105	3.25
0.088	3.50
0.074	3.75
0.062	4.00
0.052	4.25

mm	ϕ
0.044	4.50
0.037	4.75
0.031	5.00
0.026	5.25
0.022	5.50
0.019	5.75
0.016	6.00
0.013	6.25
0.011	6.50
0.0093	6.75
0.0078	7.00
0.0066	7.25
0.0055	7.50
0.0047	7.75
0.0039	8.00
0.0033	8.25
0.0028	8.50
0.0023	8.75
0.0020	9.00
0.0016	9.25
0.0014	9.50
0.0012	9.75
0.00098	10.00
0.0005	11.00
0.0003	12.00

Table 1.4 Classification of sedimentary rocks (siliciclastics and carbonates) based on grain size.

Size, mm	Siliciclastics		Carbonates				Size, mm
			Grains		Crystals		
256.0	Boulders	Conglomerate	Calcirudite*	Grain-supported	Coarsely megacrystalline	Megacrystalline	256.0
64.0	Cobbles						64.0
4.0	Pebbles						4.0
2.0	Granule				Finely megacrystalline		2.0
1.0	Very coarse sand	Sand	Calcarenite*		Very coarsely crystalline	Crystaline	1.0
0.50	Coarse sand				Coarsely crystalline		0.50
0.25	Medium sand				Medium crystalline		0.25
0.125	Fine sand				Finely crystalline		0.125
0.062	Very fine sand		Calcarenite* *(very fine grained)*		Very finely crystalline		0.062
0.031	Coarse silt	Silt			Coarsely microcrystalline	Crypto-microcrystalline	0.031
0.016	Medium silt		Calcilutite*	Mud-supported	Medium microcrystalline		0.016
0.008	Fine silt				Finely microcrystalline		0.008
0.004	Very fine silt				Very finely microcrystalline		0.004
	Clay	Clay			Cryptocrystalline		

In Russia, Pustovalov proposed the simplest and most convenient decimal classification of sedimentary rocks in 1940 (Table 1.6).

The main parameters, which characterize the pore space of clastic rocks, are the grain-size distribution coefficients. These coefficients are widely used for developing depositional models and clastic rock classifications. These coefficients are determined

Table 1.5 Particle size scale. (After Chilingar *et al.*, 1967, p. 102.)

Size, mm	Reference										Size, mm
	Krynine (1948)	Howell (1922)	DeFord (1946)		Pettijohn (1949)	Mollazal (1961)		Folk (1959, 1962)	The present authors		
4.0	Coarsely crystalline (grained)	Macro-crystalline	Mega-grained	Phaneric	Calcirudite	Macro-crystalline	Coarse	Extremely coarsely crystalline	Macrocrystalline (macrograined)	Very coarse	4.0
							Medium				
							Fine	Very coarsely crystalline		Coarse	2.0
2.0	Medium crystalline (grained)				Calcarenite	Meso-crystalline	Coarse				
1.0	Finely crystalline (grained)	Meso-crystalline	Meso-grained					Coarsely crystalline	Mesocrystalline (mesograined)	Coarse	1.0
0.5							Medium			Medium	0.5
0.25								Medium crystalline		Fine	0.25
0.1							Fine			Very fine	0.1
0.062					Calcilutite	Finely-crystalline		Finely crystalline			0.062
0.05									Finely crystalline (finely grained)		0.05
0.025											0.025
0.016								Very finely crystalline			0.016
0.01		Crypto-crystalline							Aphanic	Micro-crystalline	0.01
0.004			Micro-grained	Aphanic		Aphanic	Micro-crystalline	Aphano-crystalline			0.004
0.0025											0.0025
0.001			Crypto-grained				Crypto-crystalline			Crypto-crystalline	0.001

Table 1.6 Grain size classification of sedimentary rocks.

Rock Structure (size range)	Grain/Particle-Size Classification	Grain/Particle Size, mm
Psammitic (1.0–0.1 mm)	Coarse sand	1.0–0.5
	Medium sand	0.5–0.25
	Fine sand	0.25–0.1
Aleuritic (0.1–0.01 mm)	Coarse silt	0.1–0.05
	Medium silt	0.05–0.025
	Fine silt	0.025–0.01
Pelitic (0.01–0.0001 mm)	Coarse clay	0.01–0.001
	Fine clay	0.001–0.0001

from the cumulative frequency distribution or cumulative distribution function and include upper, middle (median), and lower quartiles of the grain-size distribution. Upper, middle (median) and lower quartiles are the arguments of the cumulative grain-size distribution function corresponding to a probability of 0.75, 0.50, and 0.25, respectively, and are designated as Q_{75}, Q_{50} and Q_{25} (Table 1.7).

The common grain-size distribution is the lognormal one, logarithm of which follows a normal or Gaussian distribution. The plot of lognormal distribution is a continuous, infinite, bell-shaped curve that is symmetrical about its geometric mean or median of a grain-size distribution. To obtain the models of the grain-size probability density curves and cumulative distribution curves, the writers used all possible combinations of three main grain-size fractions consisting of sand (1.0–0.1 mm), silt (0.1–0.01 mm), and clay (0.01–0.001 mm) particles (Figure 1.9). These models allow one to calculate the three above-mentioned quartiles or grain-size distribution coefficients.

Another two grain-size distribution coefficients (Trask, 1942) include the grain sorting index and the asymmetry of grain-size probability distribution.

Sorting index, S_0, is the probable deviation from the median grain size calculated from the cumulative grain-size distribution function:

Table 1.7 Summary of grain-pore-size and pore-throat-size measures used in conjunction with graphic analysis. (After Chilingar *et al.*, 1972, p. 353.)

Measure of central tendency:
1. *Median* (D_{50}) is the diameter which is larger than half of the pores in the distribution and smaller than the half (i.e., the middlemost member of the distribution). It reflects the overall pre size as influenced by the chemical or physical origin of the rock and any subsequent alteration. It may be a very misleading value, however.
2. *Mean* (D_M) is the measure of the overall average pore size: $$D_M = (D_5 + D_{15} + D_{25} \ldots D_{85} + D_{95})/10$$ or $$D_M = (D_{16} + D_{50} + D_{84})/3$$
3. *Mode* (D_m) is the most frequently occurring pore diameter (peak of frequency curve). If two dominant pore sizes are present which could result when there is a mixture of two or more different porosity types (vugy, oolitic, fracture, intergranular, etc.,), then the frequency curve is bimodal.
Measure of dispersion:
Pore sorting (S_p) is a standard deviation measure of the pore sizes in a sample (Folk and Ward, 1957) $$S_p = (D_{84} - D_{16})/4 + (D_{95} - D_5)/6.6$$
Measure of asymmetry:
Skewness (Sk_p) measures the non-normality of a pore-size distribution: $$Sk_p = (D_{84} + D_{16} - 2D_{50})/2\,(D_{84} - D_{16}) + (D_{95} + D_5 - 2D_{50})/2(D_{95} - D_5)$$ A symmetrical curve has a Sk_p value of 0; limits in which Sk_p varies are as follows: $-1 \leq Sk_p \leq 1$. Positive values indicate that the curve has a tail in the small pores. Negative values indicate that the curve is skewed toward the larger pores.
Measure of peakedness:
Kurtosis (K_p) is a measure of the degree of peakedness, that is, the ratio between the spread of the pore diameters in the tails and the spread of the pore diameters in the central portion of the distribution: $$K_p = (D_{95} - D_5)/2.44(D_{75} - D_{25})$$ Normal curves have a K_p of 1, whereas platykurtic (bimodal) distributions may have a K_p value as low as 0.6. A curve represented by a high narrow peak (very leptokurtic) may have K_p values ranging from 1.5 to 3.
D_n is the pore diameter in phi units as the nth percentile.
The methodology of pore- and pore-throat-size analysis (see Folk and Ward, 1957 and McCammon, 1962)

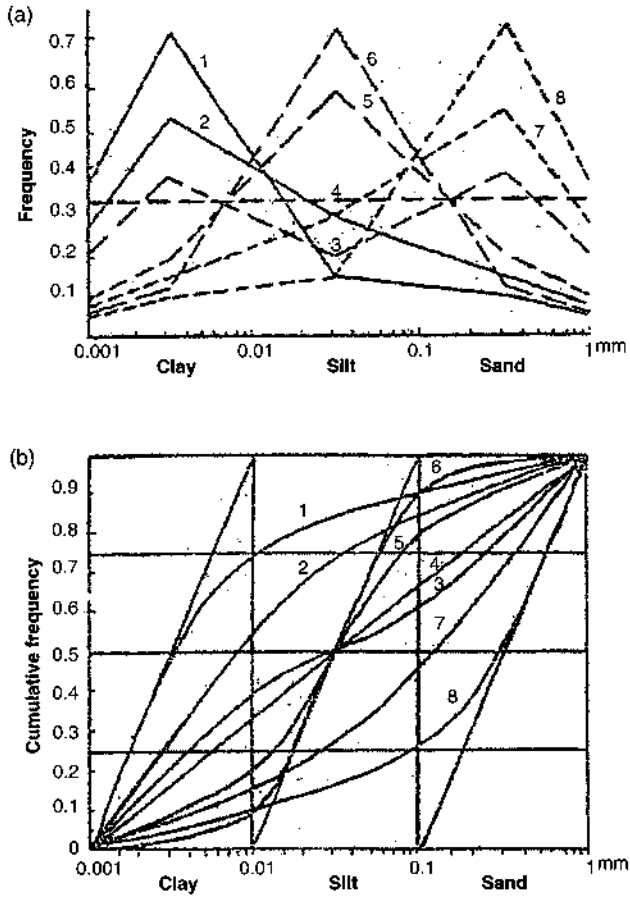

Figure 1.9 Grain-size distribution models: (a) frequency distribution, (b) cumulative frequency distribution. (Modified after Buryakovsky, 1985.). Lithology: 1–clay, 2–loam, 3–sandy-clayey poorly sorted rock, 4–unsorted rock, 5–silt, 6–sandy-clayey silt, 7–loamy sand, and 8–sand.

$$\lg S_0 = \frac{\lg Q_{75} - \lg Q_{25}}{2} \tag{1.1}$$

or

$$S_0 = \sqrt{\frac{Q_{75}}{Q_{25}}} \tag{1.2}$$

A sediment-sorting scale (Khanin, 1966) includes four classes: well-sorted sediments, S_0 = 1–1.78; medium-sorted sediments, S_0 = 1.78–2.32; poorly sorted sediments, S_0 = 2.32–2.86; and unsorted sediments, S_0 >2.86.

Asymmetry index, S_a, is calculated from the following formulae:

$$\lg S_a = \lg Q_{75} - 2\lg Q_{50} + \lg Q_{25} \tag{1.3}$$

or

$$S_a = \frac{Q_{75}Q_{25}}{Q_{50}^2} \tag{1.4}$$

When $S_a > 1$, the fine-grained material prevails, whereas when $S_a < 1$, the coarse-grained material is prevalent.

1.2.2 Pore Throat Distribution in Carbonate Rocks

Pore systems in carbonate rocks usually contain both pores and inter-connections between these pores (pore throats). Isolated vugs, however, are common in some carbonates. The pore system may have two extremes: (1) the size of the pores approaches that of the interconnecting pore throats, and (2) the size difference between the two is very large. In the mercury injection test, the size distribution between pores and pore throats is an artificial one. Mercury injection pressure is indicative of the pore throat sizes. It is usually assumed, therefore, that the pore throat sizes control the injection.

Aschenbrenner and Achauer (1960) found that both pore and pore throat sizes were essentially log-normally distributed (straight-line relationship between logarithm of pore size or pore throat size and cumulative percentage on probability paper) in Paleozoic carbonates of the Williston Basin and in the Rocky Mountains. Inasmuch as most pore- and pore-throat size distributions tend to be log-normal, this provides a method for estimating their size

Based on extensive data, Figure 1.10a illustrates a simple frequency curve showing a normal distribution with approximately 68% of the pore throat diameters occurring between D_{16} and D_{84} [one standard deviation (1.3ϕ) on either side of the mean (6.1ϕ); $\sigma_\phi = (D_{84} - D_{16})/2 = 1.3$]. Figure 1.10b illustrates the data from Figure 1.10a as a cumulative frequency curve, whereas in Figure 1.10c the cumulative frequency of pore throat sizes is plotted on Cartesian probability paper. The probability scale is designed in such a manner that a symmetrical cumulative pore-size frequency curve plots as a straight line on the graph indicating a unimodal relationship.

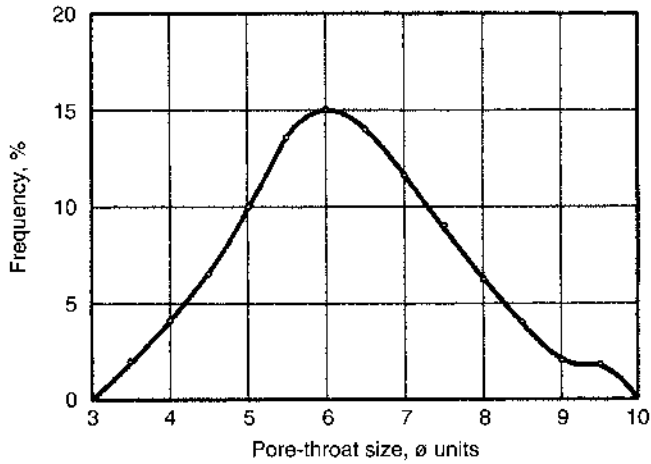

Figure 1.10a Frequency distribution of pore throat sizes in a carbonate rock.

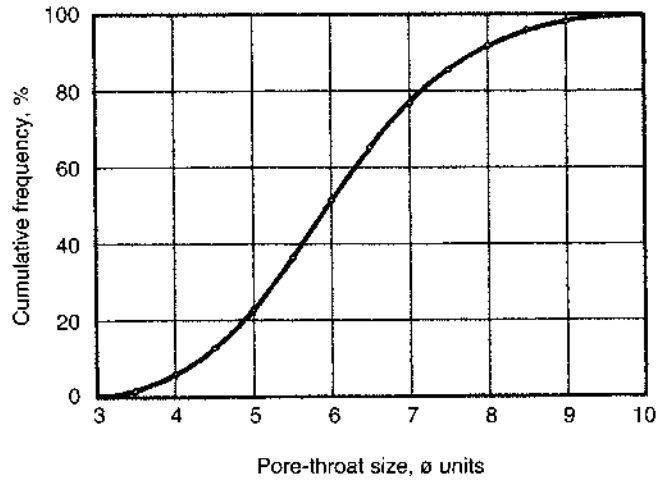

Figure 1.10b Cumulative frequency distribution of pore throat sizes (data from Figure 10a).

1.2.2.1 Cementation of Clastic Rocks

Another important characteristic of clastic rocks is their cementation while sediments become lithified or consolidated into hard, compact rocks through the deposition or precipitation of minerals in the spaces among the individual grains of the sediment. Cementation may occur simultaneously with sedimentation, or the cement may

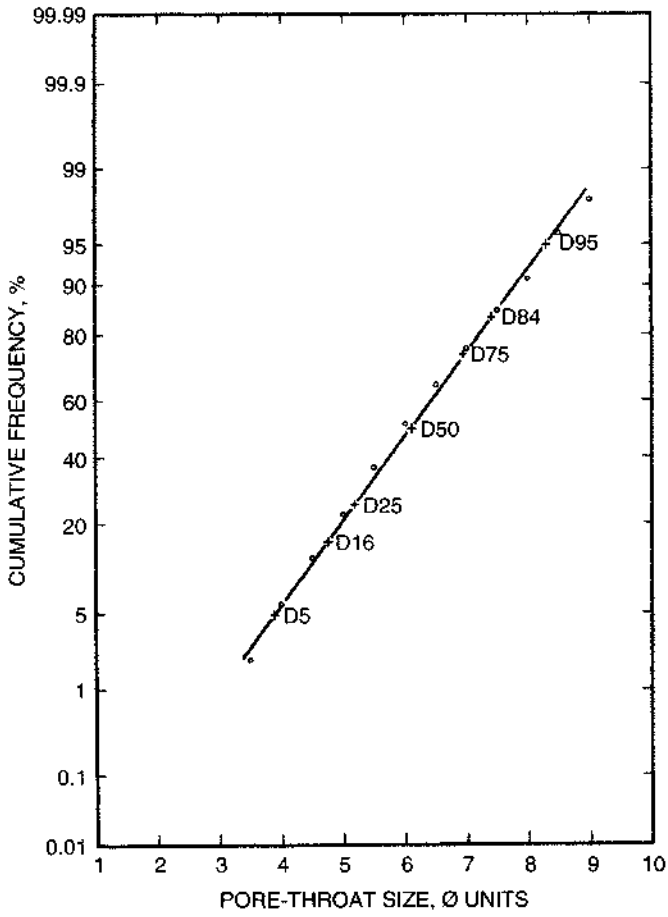

Figure 1.10c Cumulative lognormal curve on Cartesian probability paper, showing positions of various percentile ordinates (data from Figure 10a).

be introduced at a later time. The most common types of cement are silica (quartz, opal, and chalcedony), and carbonates (calcite, dolomite, and siderite). Other cements include barite, gypsum, anhydrite, and pyrite. Clay minerals constitute argillaceous cement. There are several types of cementation depending on the type of sediment supporting material: (1) mud matrix within the grain-supported sediment, including (*a*) film-like, (*b*) meniscus-like, and (*c*) pore-filling cementation; and (2) grains in a mud-supported sediment (basal cementation). Table 1.8 shows a simplified classification of clastic rock cementation.

Table 1.8 Classification of cements of clastic rocks.

Type of Cement	Content of Cement, %
Film-type	3–10
Meniscus-type	5–10
Partly pore-filling	10–20
Pore-filling	20–30
Abundant pore-filling	30–40
Basal	>40

Texture and structure of clastic rocks are the major morphologic features of a rock. Both terms are used to describe the physical appearance or geometric aspects of a rock. The term *texture* is generally used for the smaller features or particles composing a rock, whereas *structure* is used for those features that indicate the way the rock is organized or made up of its components.

Grain shape and roundness (Figures 1.11 and 1.12), grain size and sorting, grain orientation and packing, and chemical composition determine the texture of sedimentary rocks. A specific combination of these variables may reveal information about diagenetic and catagenetic processes and mechanisms acting during transportation, deposition, and compaction and deformation of sediments

Roundness is a measure of the sharpness of the particle edges, regardless of shape. One accepted method for determining roundness is to view the particles two-dimensionally, and determine the ratio of the average radius of curvature of the particle's corners to the radius of the largest circle that can be inscribed in that particle. The general method for estimating roundness is microscopic measurement of a number of grains and visual comparison to a standard chart (Figure 1.11) such as those introduced by Griffith (1967).

The degree of roundness commonly varies with size. Larger-diameter sand or gravel particles are usually more rounded than the smaller ones. Maturity and degree of weathering affect this relationship. Freshly broken fragments, which tend to be angular near the source, assume a greater degree of roundness as a result of weathering and abrasion during transportation.

Sphericity is some times confused with roundness. Although they are related in a certain degree, roundness is primarily a measurement of the angularity of a particle's corners; whereas sphericity is

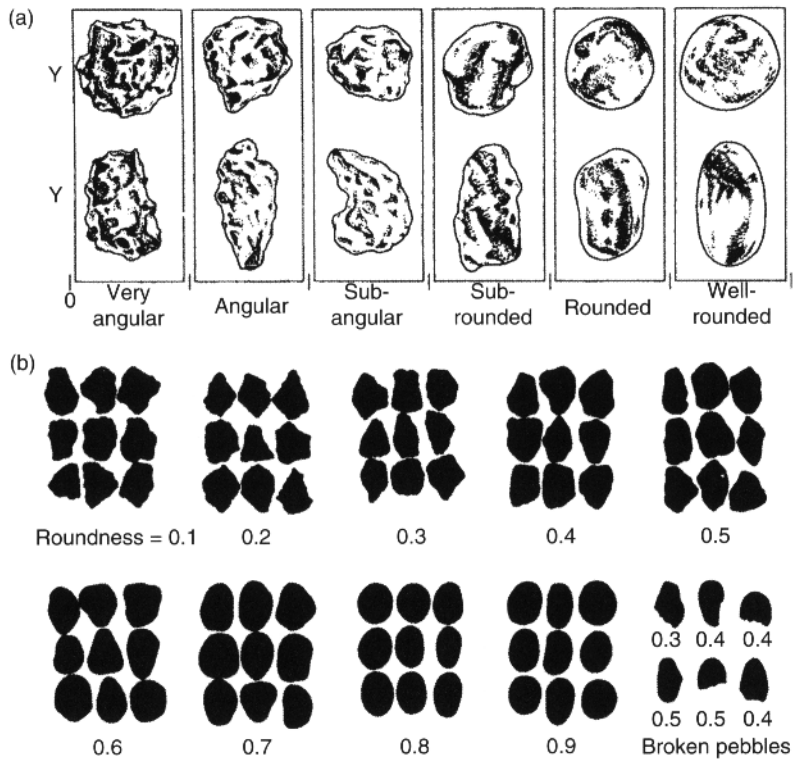

Figure 1.11 (a) *Roundness* images and classes. Columns show grains of similar roundness but different sphericity. (After Powers, 1953, modified by Pettijohn *et al.*, 1972, in Chilingarian and Wolf, 1975, p. 15, Figure 1.11.). (b) Images for estimating visual roundness. (After Krumbein, 1941, in: Chilingarian and Wolf, 1975, p.15, Figure 1.12.)

a measure of the degree the shape of the particle approaches that of a sphere. Images for estimating visual sphericity visually are given in Figure 1.12. True sphericity as defined by Wadell (1934) as the surface area of a sphere of the same volume as the particle divided by the actual surface area of the solid.

A capsule shaped object could have a roundness factor of unity, whereas if its surface area were compared to that of a sphere of the same volume, using Wadell's definition, sphericity, the ratio would be far less than unity. A more practical formula for sphericity, also introduced by Wadell (1934), is to divide the nominal diameter of the particle (the diameter of a sphere of the same volume as the particle) by the diameter by the circumscribing sphere. Krumbein

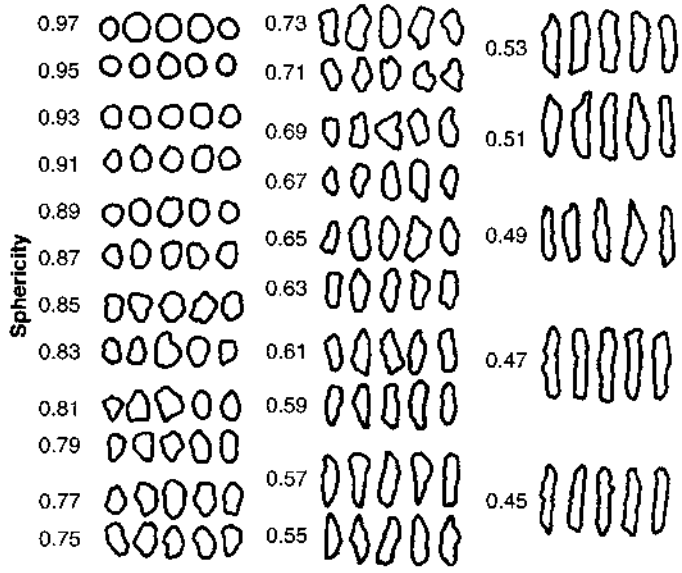

Figure 1.12 Images for estimating visual sphericity. (After Rittenhouse, 1943, in: Chilingarian and Wolf, 1975, p. 16, Figure 1.13.)

(1941) introduced a definition of sphericity based on volumes: he defined sphericity as the cube root of the volume of the particle divided by the volume of the circumscribing sphere. Factors that control the shape and roundness of particles include:

a. the original shape of the fragment,
b. durability of the fragment (hard mineral grains such as quartz and zircon are rounded less during transport than soft grains of feldspar and pyroxenes),
c. structure of the fragment (cleavage or bedding),
d. nature of the geologic agent (wind is more effective in rounding grains than water),
e. nature of the action to which the fragment is subjected and rigor of the action, and
f. residence time and distance imposed by the action.

The methods of determining parameters of rock texture and structure are the following:

1. Rock outcrop observation.
2. Core sample study.

3. Study of thin-sections under the optical microscope.
4. Study of core chips under the scanning electron microscope.
5. X-ray diffraction analysis.

A variety of structures exist in sedimentary rocks. Some of these structures formed at the time of sediment transportation and deposition. These structures are referred to as *primary sedimentary structures*. The most obvious of these is *stratification* (layering of sediments). Most layers of sediments (*strata*) accumulate in nearly horizontal sheets. Strata less than 1 cm in thickness are called *laminations*; whereas strata 1 cm or more in thickness are called *beds*. Surfaces between strata are called *bedding planes*, which represent surfaces of exposure that existed between sedimentary depositional events. Some stratification is inclined, and is referred to as *cross-stratification*.

Individual strata may also be *graded*. Normally, graded beds are sorted (becoming finer upward), a feature caused when (1) sediment-laden currents suddenly slow down as they enter a standing body of water, (2) current flow terminates, or (3) a depth of depositional basin gradually increases. In these cases, each stratum is internally graded from coarse sediments on bottom to fine sediments on top.

Many sedimentary rocks contain structures that formed after deposition. For example, desiccation cracks often form while wet deposits of mud shrink on drying. Such structures are referred to as *secondary sedimentary structures*.

Geometry of grain packing is a quantitative and qualitative presentation of the grain-packing system. Geometry of grain-packing system is very complex and depends on the specific features of grain packing and cementing. The most important geometrical parameters are the *proximity of grains*, *density of grains*, and *density of cement* of the system (Winsauer and Gaither, 1953; Kahnn, 1956).

The proximity of grains P_p is determined from the following formula:

$$P_p = q/n \cdot 100\% \tag{1.5}$$

where q is the number of grain contacts crossed by micron-scale ruler and n is the total number of grains crossed by the ruler.

Maximum proximity value may reach 100%, when all the grains are in contact with each other. Minimum (zero) value occurs when no one-grain is in contact with the others.

Generally: $0 \le q \le (n-1)$.

The density of grain compaction $P_{d\text{-}g}$ is determined from the following formula:

$$P_{d\text{-}g} = m\sum_{i=1}^{n} g_i / t \cdot 100\% \tag{1.6}$$

where m is the magnification of microscope; g_i is the number of micron-scale ruler points crossing a single grain; t is the total length of the ruler; and n is the total number of grains at all positions of the ruler.

Maximum value of the density of grains may reach 100% in the case when all ruler crossings are occupied by grains. Practically, this case is impossible for the granular (clastic) rocks.

The density of cementation $P_{d\text{-}c}$ is the relative content of cement in the rock. This parameter is calculated from the following formula:

$$P_{d\text{-}c} = \left[100 - \sum_{i=1}^{k} c_i / k\right](\%) \tag{1.7}$$

where c_i is the number of micron-scale ruler points covering i-th site of cement and k is the number of observed micron-scale ruler positions.

Except for the above-mentioned parameters, the other important parameters are (Chernikov and Kurenkov, 1977):

1. Ratio of packing proximity to the density of grains: $P_{c\text{-}g} = P_p / P_{d\text{-}g}$ (*relative compaction of grains*).
2. Ratio of packing proximity to the density of cement: $P_{c\text{-}c} = P_p / P_{d\text{-}c}$ (*relative compaction of cement*).

These parameters account for both mutual relations between individual grains and grain proportions in the rock.

Figure 1.13 illustrates one of the positions of the micron-scale ruler crossing the thin-section points on a grain, crossed by micron-scale ruler l – number of points on the cement matrix, crossed by micron-scale ruler area. Grains are counted from one side of the micron-scale ruler.

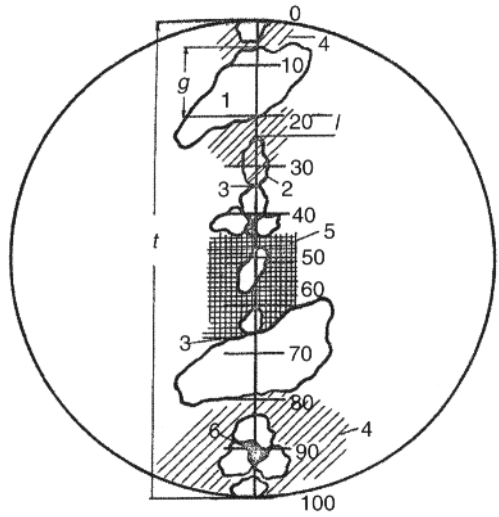

Figure 1.13 Example of microscopic image of a rock thin-section. Microscopic features: 1–quartz grain, 2–feldspar grain, 3–contact between grains, 4–argillaceous cement, 5–calcareous cement, and 6–pore space.

The grain-packing system is characterized by the following types of intragrain contacts (Taylor, 1950):

1. Point or tangent contacts – adjacent grains touch one another in a single point.
2. Linear contacts – grains connect one another through an interface.
3. Convex-concave contacts – grains are connected along the relatively smooth curve.
4. Suture contacts – grains are connected along the irregular spike-like curve.

Two other important pore-space geometrical parameters are *tortuosity* and *clearance* between the grains or in the rock matrix.

The tortuosity τ is the ratio of the effective length L_e (path of fluid flow) to the overall direction of flow, L (length of the rock sample):

$$\tau = L_e / L \tag{1.8}$$

The clearance φ is the ratio of area A_1 of openings between grains or matrix components (as are seen on the thin-section visible under the microscope) to the total area A_2 of the thin-section:

$$\varphi = A_1 / A_2 \tag{1.9}$$

Sometimes, clearance is referred to as the surface porosity. It is believed that in the absence of isolated pores, not effective for fluid flow, the product of tortuosity by clearance equals to the porosity of granular rock, i.e.,

$$\tau\varphi = \phi \tag{1.10}$$

In the presence of isolated pores, this product should be less than porosity and may be somewhat similar to the effective porosity.

1.2.2.2 *Porosity and Permeability of Clastic Rocks*

The porosity and permeability of the reservoir rocks are the most fundamental physical properties with respect to storage and transmission of fluids. Porosity of clastic rocks is controlled primarily by grain sorting (i.e., by the extent of mixing of grains of various sizes), cementation, and by the way the grains are packed together.

Porosity is at a maximum when grains are spherical and all of one size. However, porosity becomes progressively lower as the grains become more angular and pack together more closely. Artificially mixed clean sand has measured porosity of about 43% for extremely well-sorted sands, almost irrespective of grain size, decreasing to about 25% for very poorly-sorted medium-to-coarse sands; whereas the very fine-grained sands have over 30% porosity. The total porosity and bulk density of some sediments and sedimentary rocks are presented in Table 1.9.

There are four principal definitions of porosity:

a. Absolute (total) porosity, ϕ_a, ratio of the pore (void volume), V_p, to the bulk volume of sample, V_b.
b. "Effective" porosity, ϕ_{eff}, ratio of the interconnected pore volume, $V_{inter.p}$, to the bulk volume of sample, V_b. The writers prefer to call it open porosity.
c. Void ratio, e, ratio of the pore (void volume), V_p, to the grain/solids volume, V_{gr}.

Table 1.9 Total porosity and bulk density of some sediments and sedimentary rocks.

Lithology	Total Porosity, %	Bulk Density, g/cm³
Primary sediments		
Silty mud	60–70	–
Sandy mud	30–70	1.27–1.94
Lime mud	65–87	–
Clay	10–75	1.20–3.18
Clayey silt	50–60	0.80–1.80
Diatomite	30–80	0.40–1.57
Loess	30–60	1.14–1.93
Sedimentary rocks		
Sand	4–40	1.3–2.3
Sandstone	1–30	1.3–3.6
Siltstone	1–40	1.5–3.2
Shale	1–35	1.3–3.2
Sandy shale	1–25	1.8–2.9
Claystone	1–25	1.6–3.3
Marl	1–35	2.0–3.1
Chalk	10–50	1.8–2.6
Limestone	0.5–40	1.3–3.5
Dolomite	0.1–40	1.9–3.5
Anhydrite	0.2–15	2.3–3.0
Rock salt	0–5	2.1–2.3

d. Effective porosity, as proposed by the writers, is equal to the "effective" porosity as defined above (*b*) minus the irreducible fluid saturation.

Relation between the void ratio and the absolute porosity is as follows:

$$e = \phi/(1 - \phi) \tag{1.11}$$

The ease with which fluids move through the interconnected pore spaces of a reservoir rock is called permeability. Numerical

expressions of permeability are measured in Darcies (D) after Henry d'Arcy, a French engineer, who in 1856 devised a means of measuring the permeability of porous rocks. A rock has a permeability of one Darcy (1 D) when 1 cm^3 of a fluid with a viscosity of 1 cP (centipoise) flows through a 1 cm^2 of cross section of rock in 1 s under a pressure gradient of 1 atm/cm. Because most reservoir rocks have an average permeability considerably less than one Darcy, the usual measurement is in millidarcies (mD), i.e., one thousandth of a Darcy.

The magnitude of permeability depends on wettability, i.e., on whether (1) the fluid does not wet the solid surfaces of the rock and, therefore, occupies the central parts of the pores, or (2) the fluid wets the solid surfaces and thus tends to concentrate next to the rock surfaces and in smaller pores. The nature, distribution, and amount of immobile phase affect the effective permeability. The effective permeability as defined by the writers is the permeability of a core containing an irreducible fluid.

The relative permeability to a fluid is defined as the ratio of effective permeability at a given saturation of that fluid to the absolute permeability at 100% saturation. The terms $k_{ro}(k_o/k)$, $k_{rg}(k_g/k)$, and $k_{rw}(k_w/k)$ denote the relative permeability to oil, to gas, and to water, respectively (k is the absolute permeability, often a single-phase liquid permeability). The relative permeability is expressed in percent or as a fraction.

In waterflooding projects or in natural water-drive pools, the relative permeability to oil and to water is of great importance. Where water and oil flow together, the relative permeability is affected by many factors, which include (1) relative dispersion of one phase in the other, (2) time of contact with pore walls, (3) amount of polar substances in the oil, (4) degree of hardness of water, (5) relative amount of carbonate material in porous medium, and (6) temperature knowledge of the distribution of porosity and permeability is required for the efficient development, management, and prediction of future performance of an oilfield.

1.2.3 Carbonate Rocks

Carbonate rocks represent a complex group, which is difficult to study. The carbonate rocks include limestones composed mostly of calcite ($CaCO_3$) and dolomites, containing both calcium and magnesium [$CaMgCO_3)_2$].

Limestone is composed of more than 50% carbonate minerals; of these, 50% or more consist of calcite and/or aragonite. A small admixture of clay particles or organic matter imparts a gray color to limestones, which may be white, gray, dark gray, yellowish, greenish, or blue in color; some are even black. Dolomites are rocks, which contain more than 50% of the minerals dolomite and calcite (plus aragonite), with dolomite being more dominant. The pure dolomite mineral is composed of 45.7% $MgCO_3$ and 54.3% $CaCO_3$, by weight; or 47.8% CO_2, 21.8% MgO, and 30.4% CaO. Dolomites are quite similar to limestone in appearance and, therefore, it is difficult to distinguish between the two with the naked eye. On the basis of CaO/MgO ratios, Frolova (1959) proposed the classification presented in Table 1.10. The origin, occurrence, classification, and physical and chemical aspects of carbonate rocks are presented in detail by Chilingar *et al.* (1967a,b).

It is very important to evaluate as correctly as possible various properties of carbonate rocks. A good case in point is the Fullerton Clearfork dolomitic limestone reservoir in the Permian Basin. Bulnes and Fitting (1945) reported that 82% of the core samples had permeability of less than 1 mD. The problem of what to use for minimum productive permeability becomes very acute in such instances. According to Bulnes and Fitting, if 1 mD were used as the minimum productive permeability instead of the actual value of 0.1 mD, the resulting estimated ultimate recovery would be 70% in error. The core analysis of some carbonate rocks is complicated by the presence of fractures and solution cavities. In order to analyze such rocks, "whole" or "large" core analysis, whereby the entire core is analyzed instead of small plugs, was developed.

Dunham proposed an excellent classification of limestones in 1962 on the basis of their texture and mud content. Limestones which are composed of particles of less than 2 mm in size and which retained their original, depositional texture can be classified as follows:

1. Lime mudstone with less than 10% grains in a mud-supported sediment.
2. Lime wackestone with more than 10% grains in a mud-supported sediment.
3. Lime packstone with mud matrix within the grain-supported sediment.

Table 1.10 Frolova's classification of dolomite-magnesite-calcite series. (After Frolova, 1956, p. 35.)

Name	Content, %			CaO/MgO Ratio
	Dolomite	Calcite	Magnesite	
Limestone	5–0	95–100	...	>50.1
Slightly dolomitic limestone	25–5	75–95	...	9.1–50.1
Dolomitic limestone	50–25	50–75	...	4.0–9.1
Calcitic dolomite	75–50	25–50	...	2.2–4.0
Slightly calcitic dolomite	95–75	5–25	...	1.5–2.2
Dolomite	100–95	0–5	...	1.4–1.5
Very slightly magnesian dolomite	100–95	...	0–5	1.25–1.4
Slightly magnesian dolomite	95–75	...	5–25	0.80–1.25
Magnesian dolomite	75–50	...	25–50	0.44–0.80
Dolomite magnesite	50–25	...	50–75	0.18–0.44
Slightly dolomitic magnesite	25–5	...	75–95	0.03–0.18
Magnesite	5–0	...	95–100	0.00–0.03

4. Lime grainstone with no mud matrix within the grain-supported sediment.
5. Lime boundstone in which original components are bound together.

The following two types of limestones are distinguished, if they are composed of particles of less than 2 mm in size and in which the depositional texture has been destroyed by recrystallization,

1. Crystalline limestone with a fine texture.
2. Sucrosic ("sugary") limestone with a coarse texture.

Embry and Clovan (1971) expanded Dunham's classification to include limestones containing more than 10% of the clasts larger than 2 mm in size (coarse clasts):

1. Floatstone with coarse clasts in the matrix-supported sediment.
2. Rudstone with coarse clasts in the clast-supported sediment.

Carbonates are quite different from siliciclastic rocks, especially because of their susceptibility to post-depositional changes, particularly dolomitization involving the action of magnesium-bearing water (seawater or percolating meteoric water). Chemical equation explaining the molecular replacement of limestone by dolomite was proposed by Elie de Beaumont in 1836 as follows:

$$2CaCO_3 + MgCl_2 \rightarrow CaMg(CO_3)_2 + CaCl_2$$

Chilingar and Terry (1954) showed that a definite relationship exists between porosity and degree of dolomitization as exhibited in the Asmari Limestone in Iran (Chilingar *et al.*, 1972; Sarkisyan *et al.*, 1973).

T. F. Gaskell of the British Petroleum Co. Ltd. (personal communication, 1963) determined the porosity and density of carbonate reservoir rocks in Southwestern Iran. The average density values for the different oilfields, grouped in ranges of porosity of 0–4.0%, 4.1–8.0%, 8.1–12.0%, and >12.1% are presented in Table 1.11. The mean values were weighted according to the number of observations for each oilfield. A certain amount of the density scatter may be due to impurities in the limestones, variation in the degree of secondary cementation subsequent to dolomitization, and so on. The gradual trend of density from 2.70 g/cm^3 at low porosity to 2.80 g/cm^3 for the high-porosity group indicates that dolomitization gives rise to porosity (Figure 1.14). Inasmuch as at 20°C the density of calcite is 2.71 g/cm^3 and that of dolomite is 2.87 g/cm^3, the average values given in Table 1.11 correspond to the percentage of dolomitization given in Table 1.12. These results are in close accord with those obtained by Chilingar and Terry (1954). This relationship also presents the possibility of determining porosity from matrix density of drill chips and grains.

Table 1.11 Relationship between porosity and specific gravity of Iranian carbonate rocks (Asmari Limestone).

Oil Field	Porosity Range*(%)							
	0–4.0		4.1–8.0		8.1–12.0		≥ 12.1	
Haft Gel	2.68 ± 0.04	(14)	2.73 ± 0.09	(9)	2.75 ± 0.14	(8)	2.68 ± 0.12	(20)
Naft Khaneh	2.62 ±	(1)	2.77 ± 0.08	(3)	2.81 ± 0.05	(9)	2.83 ± 0.05	(24)
Gach Saran	2.71 ± 0.09	(7)	2.77 ± 0.08	(10)	2.78 ± 0.08	(11)	2.79 ± 0.08	(8)
Agha Jari	2.74 ± 0.09	(7)	2.74 ± 0.09	(10)	2.73 ± 0.06	(5)	2.81 ± 0.09	(9)
Naft Sefid	2.67 ± 0.04	(3)	2.73 ± 0.04	(3)	2.76 ± 0.06	(9)	2.76 ± 0.09	(12)
Lali	2.74 ± 0.08	(6)	2.74 ± 0.03	(6)	2.79 ± 0.04	(3)	2.79 ± 0.03	(4)
M-i-S	2.67 ± 0.12	(11)	2.71 ± 0.11	(8)	2.73 ± 0.12	(9)	2.80 ± 0.06	(12)
Mean	2.70 (49)		2.74 (49)		2.76 (53)		2.80 (89)	

*The ± figures are mean square errors of the average values, and the figures in parentheses are the numbers of observations.

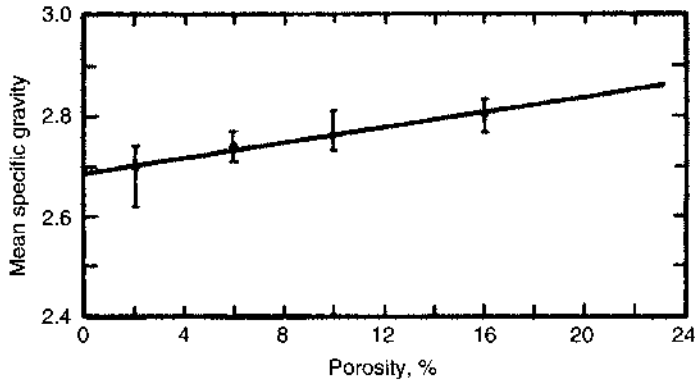

Figure 1.14 Relationship between specific gravity and porosity of Iranian carbonate rocks (Asmari Limestone). (After T.F. Gaskell, British Petroleum Co, Ltd. Personal communication, 1963.)

Table 1.12 Relationship between porosity and density of Asmari Limestone in Iran.

Porosity (%)	Specific Gravity	Dolomitization (%)
0–4.1	2.70	0
4.1–8.0	2.74	20
8.1–12.0	2.76	32
≥ 12.1	2.80	58
	2.84	82

As in the case of siliciclastic rocks, carbonate rocks that had higher initial porosity, underwent the most extensive diagenetic changes. It should be noted that lithification of carbonates rocks takes place much faster than that of sandstones and siltstones. This results in an earlier completion of the process of mechanical compaction.

More than thirty different natural processes, which are controlled by local and regional factors, occur during the diagenesis and catagenesis of carbonates (Chilingar *et al.*, 1979; Larsen and Chilingar, 1983). Lithification of carbonate sediments is of biochemical, physicochemical, and mechanical nature. To some extent, these processes occur simultaneously and change both the composition and the pore geometry of sediments and rocks. With time, their rates are reduced.

An essential difference between mechanical and biochemical – physicochemical processes is that the former acts in one direction with results being mostly irreversible. Biochemical and physicochemical processes, on the other hand, can take place in different directions; thus, increase and decrease in secondary porosity of carbonate rocks can occur periodically depending on the environmental conditions. Inasmuch as the mechanical processes are unidirectional and usually irreversible, possibly they play a major role in changing the original (primary) porosity of carbonate rocks. Thus, there is similarity with compaction of terrigenous (siliciclastic) rocks.

Degree of consolidation, dissolution and cementation under the overburden pressure is important. Increase in overburden load as a result of subsidence of sediments leads to the solution of crystals under pressure, i.e., differential solution takes place in more strained parts of grains with a subsequent deposition of material on the surfaces having lower potential energy. In addition, grains (and crystals) may get flatter parallel to the surface of stratification. These processes decrease the initial porosity of carbonate rocks.

Carbonates can be also extensively fractured. In this situation, even without porosity and permeability in the main body of the formation, commercial amount of oil can exist.. On the basis of fracture width, fractures can be classified into:

1. *supercapillary* (width greater than 0.26 mm),
2. *capillary* (width from 0.26 to 0.0001 mm), and
3. *subcapillary* (width less than 0.0001 mm).

Mar'enko (1978) proposed another classification of fractures, but the writers prefer the following classification:

1. fine macrofractures (width = 1 – 10 mm),
2. fine fractures (width = 0.1 – 1 mm),
3. very fine fractures (width = 0.01 – 0.1 mm),
4. hair-thin fractures (width = 0.001 – 0.01 mm), and
5. microfractures (width = 0.0001 – 0.001 mm).

Subsequent dissolution may enlarge initial fractures and, thus, increase fracture porosity as shown in Figure 1.15. Often, one can observe vugs along the extent of fractures. In carbonates, the porosity, permeability, and pore space distribution are related to both

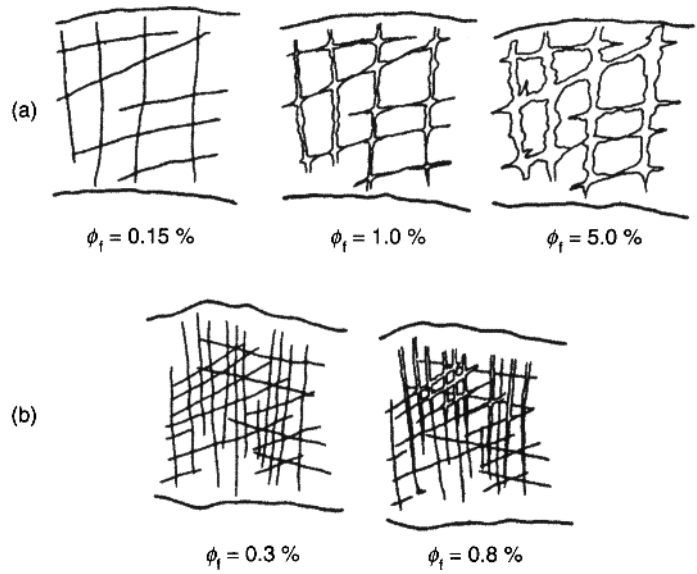

Figure 1.15 Development of fracture porosity in carbonate reservoir rocks that have (a) low insoluble residue (IR) content and (b) high IR content. (After Tkhostov *et al.*, 1970, Figure 11.)

the depositional environment of the sediment and the changes that have taken place after deposition. When volume loss occurs due to solution and recrystallization, irregular voids are formed called vugs (vuggy porosity).

The initial porosity of carbonates often approaches that of sandstones in that their structure consists of aggregates of oolites, grains, and crystals. The initial (primary) porosity of carbonates depends on their genetic type to a great extent: it is the largest in biogenic and clastic (detrital) varieties, whereas it is considerably lower in cloddy and chemogenic ones (excluding chemogenic oolitic limestones). According to Aksenov *et al.* (1986), values of maximum porosity of carbonate rocks considering their structural-genetic types are: biogenic – 24%, biogenic-detrital – 24%, clotted-cloddy – 13%, crystalline-granular – 4%, pelitomorphic – 2%, and oolitic and pisolitic – 24%.

Permeability is controlled by the size of the passages (pore throats) between the much larger pores and vugs. Mercury injection into the rock pore space in the laboratory measures the size of pore throats rather than those of the void space. Consequently, a highly porous rock may have little or no permeability if these

interconnections are very narrow or absent. On the other hand, some very fine-grained carbonate rocks have an extensive network of interconnected pore space with enough permeability to be able to yield commercial volumes of oil. Intercrystalline pores tend to be interconnected, and rocks with high intercrystalline porosity are normally permeable as found in many highly-productive dolomite reservoir rocks.

Studies are continuing on the effects of post-sedimentation processes on the properties of carbonate reservoir rocks (e.g., see Sarkisyan *et al.*, 1973). Many good bioclastic carbonater reservoir rocks (i.e., high porosity and permeability) originate in the shallow parts of the basins. Sulfatization, calcification, and silicification affect adversely the reservoir-rock properties. The secondary mineralization processes, however, indirectly improve the flow capacity of rocks (permeability) by creating heterogeneity, which favors the subsequent formation of fractures and solution cavities. Dolomitization, in general, either creates or increases porosity.

Bioherms. Considerable attention is paid to the origin of bioherms and reefs and the properties of composing rocks, mainly because of practical considerations. Many carbonate reservoirs are present in reefs and bioherms.

Korolyuk and Mikhaylova (1970) presented an elaborate classification of bioherms and reefs. They defined *organic structure* as a geologic body formed as a result of growth on each other of attached or colonial organisms together with the complex of associated rocks (Figure 1.16). During certain periods of their growth, various organic structures could have been "wave breakers". Biorhythmites are characterized by repeated occurrence of bioherms, biostromes, and other related bodies in the sequence of bedded rocks.

The classification of Korolyuk and Mikhaylova (1970) is based on lithologic-morphologic principles rather than paleogeographic ones (Figure 1.16, 1.17, 1.18, and 1.19). Korolyuk and Mikhaylova (1970) recognized the following three types of reef complexes: I – Reef complex that is composed of organic core and greatly subordinate, low-volume, flanking organo-detrital deposits. II – Reef complex that includes massive organic structure with adjoining, detrital, flanking deposits; the volume of flanking deposits (fore-reef and back-reef) is smaller than that of the core. Among detrital rocks, coarse-detrital varieties play a major role. III – Reef complex that includes small organic core and much more massive (voluminous) flanking deposits (various rocks).

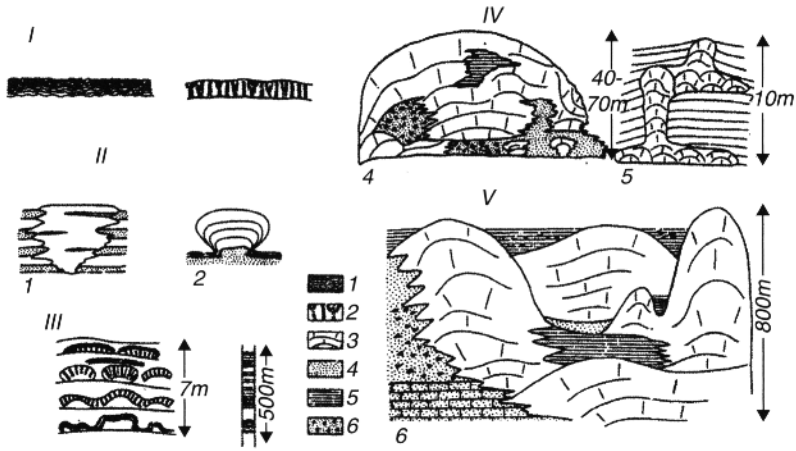

Figure 1.16 Types of organic structures. (After Korolyuk and Mikhaylova, 1970, Figure 1, p. 230.) I – Biostromes, 0.5 – 5 m thick and 10 – 100 m long; II – bioherms, oncoids, 1 – 10 m; III – biorhythmites; IV – biohermal massive, 10 – 100 m; and V – reef massive, hundreds of meters 1 – Archaeocyathidal bioherms, Cambrian, western Siberia (after I.T. Zhuravleva) (arrested growth); 2 – stromatolitic bioherms. Cambrian, western Siberia (free-growing); 3 – stromatolitic biorhythmites, Cambrian, western Siberia; 4 – biohermal massive, Jurassic, western Crimea; 5 – biohermal massive, Sarmatian, Moldavia; and 6 – reef massive , Jurassic, Caucasus Lithology; 1 – bedded stromatolites; 2 – columnar stromatolites; 3 – biohermal massive limestones; 4 – organo-clastic limestones; 5 – chemical carbonates; and 6 – coarse detrital limestones.

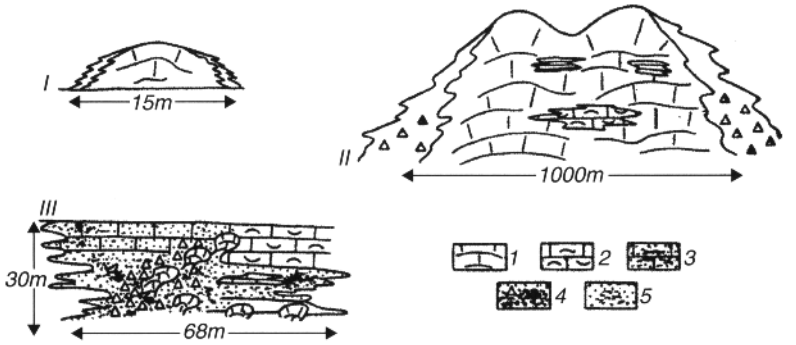

Figure 1.17 Types of reef complexes. (After Korolyuk and Mikhaylova, 1970. Figure 2, p. 231.) I – Stromatolitic-bryozoan bioherm, Ordovician, Baltic region; II – reef massive, Upper Jurassic, Crimea; and III – reef complex, Upper Jurassic, western Crimea. Lithology: 1 – biohermal limestone; 2 – organic-detrital limestone; 3 – fine-detrital limestone; 4 – limestone breccia; and 5 – limestone gravels and sandstones.

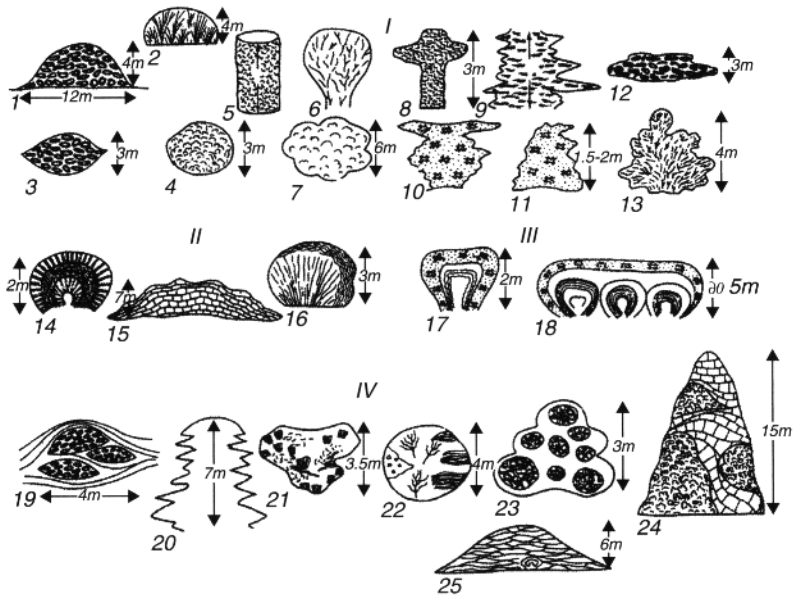

Figure 1.18 Types of bioherms. (After Korolyuk and Mikhaylova, 1970. Figure 3, p. 231.) 1 – Simple homogeneous; II – simple zonal; III – complex zonal; and IV – complex spotty. 1 – Archaeocyathidal, Cambrian, western Siberia (after I.T. Zhuravleva): 2 – coralline, Devonian, northern Caucasus; 3 – Archaeocyathidal-algal, Cambrian, Tuva; 4 – renaltsician, Cambrian, western Siberia (after I.T. Zhuravleva); 5 and 8 – bryozoan-nubecularian, Sarmatian, Moldavia (after V.S. Sayanov); 6 – coralline, Jurassic, western Crimea; 9 – algal, Jurassic, Crimea; 10 and 11 – bryozoan, Neogene, Ukraine (after L.A. Belokrys); 12 – Archaeocyathidal-agal, Cambrian, Altay (after V.D. Fomin); 13 – bryozoan, Neogene, Kerch; 14 – stromatolitic, Cambrian, western Siberia; 15 – *Rhodophyceae* (algal), Jurassic, Crimea; 16 – bryozoan, Neogene, Crimea, ; 17 and 18 – bryozoan algal (Rhodophyceae), Neogene, Crimea (after L.A. Belokrys); 19 – Archaeocyathidal, Cambrian, Siberia (after I.T. Zhuravleva); 20 – coralline-stomatoporan, Devonian, Novaya Zemlya (after Patrunov); 22 – coralline-algal, Jurassic, Crimea; 23 – serpulo-bryozoan, Neogene, western Crimea, and 24 – coralline-bryozoan, Jurassic, Crimea.

Bioherms were divided into four types: I – Homogenous bodies constructed by one or two types of organisms (e.g., coralgal and bryalgal), with minor admixture of other organic limestones. II – Zonal bioherms composed of one or two frame-building organisms, systematically close to each other. III – Zonal bioherms composed of several remotely related frame-building organisms, but occurring in regular layers. IV – Complex, spotty bioherms formed by several frame-builders, distributed in clusters and, as a rule, accompanied

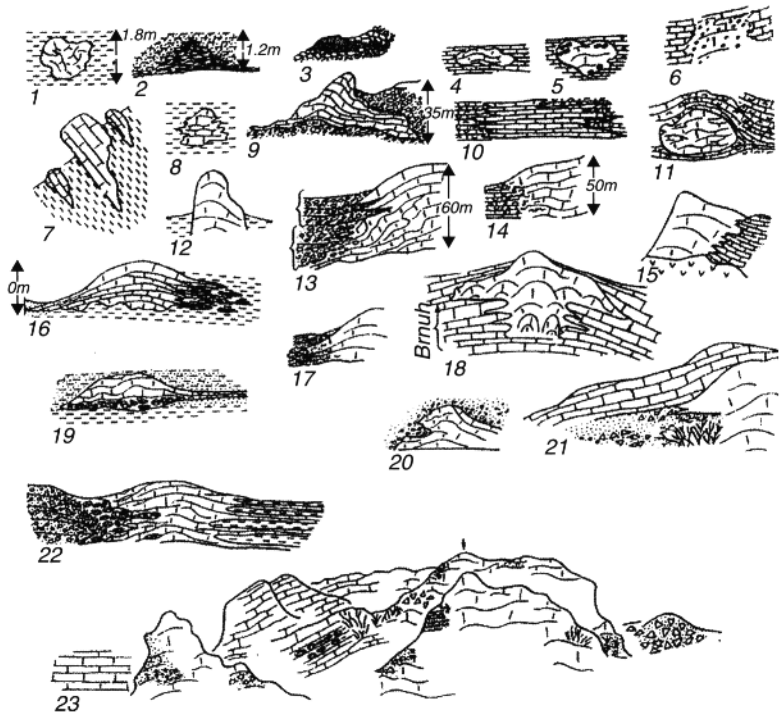

Figure 1.19 Types of contacts of organic structures. (After Korolyuk and Mikhaylova, 1970, Figure 4., p. 233.) 1-11 – *Small forms*: 1 – Upper Oxfordian, Sudak area, Crimea; in clays, butt-joint; 2 – Upper Oxfordian; Lysaya (Bold) Mountain, Crimea; in clay, butt-joint; 3 – Oxfordian, Panagiya landmark, Crimea; in sands and conglomerates, growth; 4 – Upper Devonian, Frontal Ridge of Northern Caucasus (after S.M. Kropachev and I.V. Krutu); in limestones, butt-joint; 5 – Neocomian, Crimea (after E.I. Kuz'micheva); in limestones; 6 – Silurian, Vaazalemma, Estonia; in limestones, intergrowth; 7 and 8 – Permian, Darvaz (after M.A. Kalmykova) in clays, wedging-in; 9 – Oxfordian, Panagiya landmark, Crimea, in sands and conflomerates, butt-joint; 10 – Kimmeridgian, Karaba-Yayla, Crimea, in limestones, wedging-in; and 11 – Oxfordian, Delyamet-Kaya, Crimea, in limestones, enveloping. Twelve to twenty two – *biohermal massives*: 12 – Upper Oxfordian, Sakharnaya Golovka (Sugar Head), Crimea; in clays; 13 – Oxfordian, Khart-Kaya, Crimea: in sandstones and conglomerates; complex, upper part – wedging-in, lower part –intergrowth; 14 – Oxfordian-Kimmeridgian, Redant, northern Caucasus; in limestones, gradual; 15 – Oxfordian- Kimmeridgian, Georgia (after N.S. Bendukidze); in limestones, wedging-in; 16 – Upper Oxfordian, Lysaya (bold) Mountain, Crimea; in clays, complex and gradual wedging-in (right side); 17 – Upper Oxfordian, Fiagdon River, Northern Caucasus; in sandstones and conglomerates, complex envelopment and intergrowth; 18 – Samatian, Pogornichany, Moldavia (after V.S. Sayanov); in limestones, upper part – complex envelopment, lower – wedging-in; 19 – Upper Oxfordian, Likon Mountain, Crimea, in clays, left side – lens-like wedging-in, right side – butt-joint and gradual; 20 – Upper Permian, Abago Range, Greater Caucasus (after A.A. Belov; in sandstones and conglomerates, complex, erosion and envelopment; 21 – Oxfordian- Kimmeridgian, Gizeldon River, Northern Caucasus; in limestones; 22 – Kimmeridgian, Demirdzhi Yayla Mountain (center), Crimea; in clays; and 23 – Oxfordian-Kimmeridgian reef massive, Oshtein Mountain (arrow); Glavnyy (main) Caucasus Range.

by a rich variety of other organisms. The role of non-biohermal deposits (detrital, etc.) is significant.

1.2.4 Carbonate versus Sandstone Reservoirs

Around sixty five percent of World oil reserves reside in carbonates. Unfortunately, the recovery factor from carbonates is much lower than those from sandstone reservoirs. Thus, an all-out effort should be made to correct this unfortunate situation. Some of the reasons for this sad situation can be summarized as follows:

1. Greater heterogeneity of carbonate reservoir rocks compared with sandstones. Often, heterogeneity can be observed even on a thin-section scale.
2. Carbonate rocks appear to be more oil-wet than water-wet compared with sandstones.
3. The presence of fractures adds new dimension to be fluid flow problems.
4. The presences of double porosity system [i.e., low-permeability matrix and fractures (including vugs)] results in very low recoveries. The greatest challenge is to how to move the oil from the low-permeability matrix into the fractures. Most of the flow occurs in fractures.
5. In carbonates that have intergranular porosity, permeabilities parallel and perpendicular to the bedding are about equal, whereas in sandstones the horizontal permeability is much greater than the vertical permeability.
6. Tectonically caused overpressures in lithified carbonates defy the existing predictive techniques.

1.2.5 Volcanic/Igneous Rocks

Fractured volcanic rocks occasionally play an important role in creating reservoirs and traps for hydrocarbon accumulation. Reserve estimation in such traps requires sophisticated methods of studying reservoir rock properties, such as density of fractures, specific surface area, width of fractures, irreducible fluid saturation, pore space structure, porosity, and permeability (Kondrushkin and Buryakovsky: 1987; Abasov *et al.*, 1997).

As an example, the productive volcanic Muradkhanly Oilfield (Figure 1.20) in the center of the Kura Depression, Azerbaijan, is described here. Reservoirs have been formed in the weathered volcanic rocks of the upper portion of Upper Cretaceous section. Oil traps here were formed by transgressive overlapping by Maikop shales in the shallowest part, and by Eocene terrigenous-carbonate rocks on the western flank. Commercial oil reserves are associated with the fractured Upper Cretaceous volcanic rocks. Productivity of the Eocene terrigenous, carbonate, pyroclastic rocks, and the Middle Miocene terrigenous-carbonate rocks encountered in this field is lower than that of the Upper Cretaceous volcanic rocks.

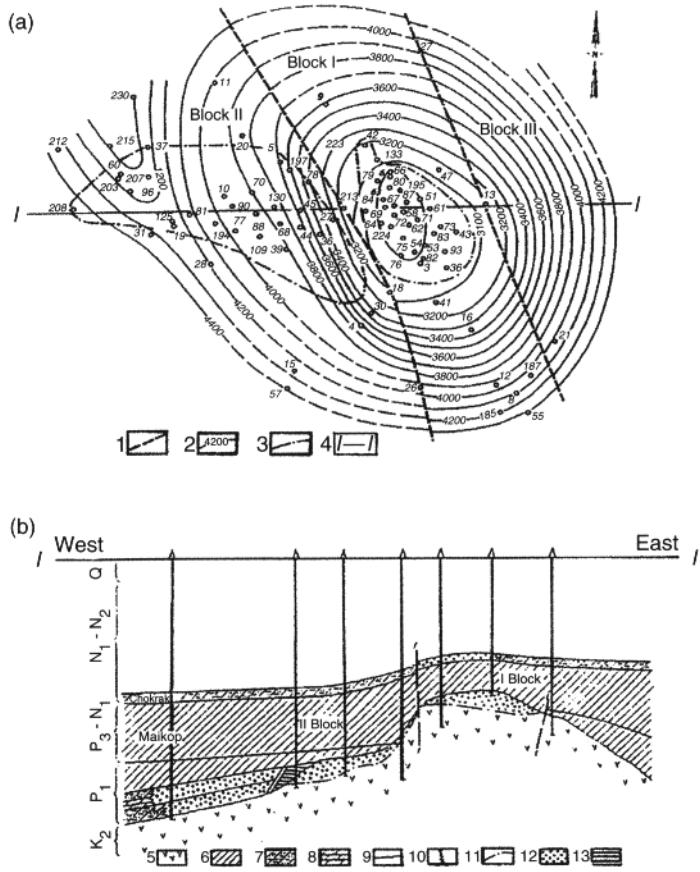

Figure 1.20 Muradkhanly Oilfield: (a) structural map on the top of volcanic rocks; (b) cross-section along the line west to east I – I. (Modified after Buryakovsky *et al.*, 2001.) 1–Faults; 2–Contour lines on top of volcanic rocks; 3–initial OWC; 5–volcanic rocks; 6–clay/shale; 7–alternation of sand, silt and shale; 12–oil reservoir.

Logs from the Muradkhanly Oilfield indicate that an anticline is present above the volcanic rocks at a minimum depth of 3000 m. Within the 4200-m contour line, the overall field size is 15 × 11 km. The dips vary from 10 to 20°. The structure is cut by two faults and, hence, is divided into three separate blocks (Figure 1.20). Oil reserves are concentrated in the crestal area (Block I) and at the western flank of the structure (Block II).

The Upper Cretaceous includes undisturbed volcanic rocks: pyroxene-andesite; biotite-, hornblende, and pyroxene-trachyandesite; porphyry and amygdaloidal basalts; and products of alteration due to weathering of volcanic rocks with admixture of clastic material (tuff-sandstones, tuff-breccia, and tuff-gritstone; also see Figure 1.21). Penetrated thickness of sedimentary and volcanic rocks ranges from 3 to 1952 m.

The porosity of volcanic rocks is of fracture-vuggy and intergranular type. Large intergranular pores, vugs and fractures are present in the core samples. Large pores are 1 mm (average) in diameter, whereas vugs have diameters of 2 cm (average). Microfractures, which contain mainly calcite and argillaceous cement, have widths of ≥ 0.1 mm. Oil is present in large intergranular pores, vugs, and fractures. During drilling, lost circulation (up to 100 m^3/d) and high oil flows (up to 500 metric tons per day) in several wells suggest that there are long and wide fractures in the volcanic rocks.

Microfractures have been studied in 4 × 5 cm thin-sections. Microscopic fracture porosity ranges from 0.04 to 0.004%, fracture

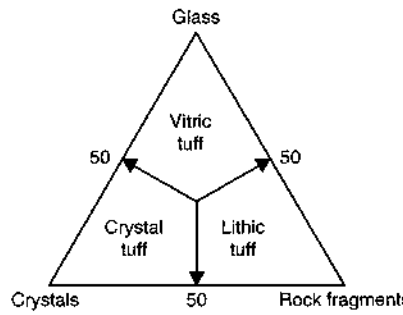

Figure 1.21 Triangular diagram and end members of tuffs. (After Pettijohn *et al.*, 1972, Figure 7-9, p. 269; see O'Brien, 1963; Fisher, 1961; courtesy of Springer-Verlag, New York).

permeability varies from 0.16 to 6.90 mD, and average fracture density (total length of fractures per unit area) is 0.30 cm/cm^2.

Scanning Electron Microscope (SEM) micrographs show that the volcanic rock texture depends on the original properties of the unweathered rocks with subsequent imprint of weathering. Oil flows (up to 500 t/d) in several wells suggest that there are long and wide fractures in the volcanic rocks.

Petrographic studies show that reservoir properties depend on the degree of weathering of volcanic rocks. The formation of large pores and vugs is due to the plagioclase dissolution. Sometimes, when plagioclase and other minerals are dissolved, micro-caverns are formed.

Microfractures have been studied in 4 × 5 cm thin-sections. Micro-fracture porosity ranges from 0.04 to 0.004%, fracture permeability varies from 0.16 to 6.90 mD, and average fracture density (total length of fractures per unit area) is 0.30 cm/cm^2.

Scanning Electron Microscope (SEM) micrographs show that the volcanic rock texture depends on the original properties of the unweathered rocks with subsequent imprint of weathering and alteration. Alteration of ash resulted in the formation of such clay minerals as smectite (montmorillonite), chlorite and biotite during diagenesis and catagenesis. Secondary matrix pores vary in size from 1 to 200 μm. Pores are often connected by irregularly curved fractures, 10–600 μm long and 0.5–10 μm wide.

Mercury injection studies show that the volcanic rock matrix within the unproductive and/or low-productive sections contains up to 60–75% of small pores with radii less than 0.1 μm, i.e., sub-capillary pores not involved in fluid migration. Diameters of pore throats, which are important for fluid movement, range from 0.25 to 6.3 μm. A power-law correlation between the pore throat diameter and matrix (intergranular) permeability is as follows:

$$k = 0.0525 d_{ch}^{2.85} \tag{1.12}$$

were k is the permeability in mD and d_{ch} is the pore throat diameter in μm.

The porosity of volcanic rocks studied in core samples by the saturation method varies within a wide range (0.6 to 28%), with an average value of 13%. The intergranular permeability is low; it varies from 0 to 10 mD, with an average value of 1 mD. The unusual combination of high porosity and very low permeability is explained by

the complex and non-uniform structure of the porous space. Finely-porous rocks have complex pore structure and curved channels. The 0.1-μm subcapillary pores are not involved in fluid migration. The secondary matrix porosity includes pores (0.25 μm up to 1 mm in size) and vugs (larger than 1 mm in size). Commonly, these pores and vugs are partly filled with kaolinite, illite, smectite (montmorillonite), ferro-oxides, and zeolites; some clays are dispersed and highly swelling. Clay mineral content (mainly authigenic) in rocks is variable and can reach 40% or more. The petrophysical study shows that if the content of highly-dispersed clay is more than 40%, then the water saturation of rocks is almost 70% and even higher. Under these conditions, rocks cannot be considered productive.

Oil is present both in the rock matrix (pores and vugs) and in the micro- and macro-fractures. The intergranular matrix permeability is very low, and the oil saturation of reservoir rocks is distributed unevenly. Oil is produced mainly from zones that have hydrodynamic connections with the fracture systems. For quantitative evaluation of volcanic reservoirs, core samples from inside-perimeter wells with oil production and outside-perimeter wells without fluid flow were analyzed. The two statistical distributions of porosity were compared, and the average porosity values were determined. The secondary porosity (ϕ_1) (vugs and fractures) can be determined using the following formula:

$$\phi_1 = (\phi_2 - \phi_3)/(1 - \phi_3) \tag{1.13}$$

where ϕ_2 is the porosity within the productive zones in the inside-perimeter wells and ϕ_3 is the porosity within the unproductive zones in the outside-perimeter wells.

The average secondary porosity is 1.8%. Depth intervals with high porosity (the secondary pores, vugs, and fractures) were determined using log data (electrical, radioactive, sonic, and caliper) and well test data. Thickness of these intervals can be considered as the effective (oil-bearing) reservoir thickness (net pay). These intervals have been identified using porosity determined from log data. Two porosity cut-off limits were identified:

1. Lower limit: for impermeable, unproductive rocks, porosity is less than 7–8%.
2. Upper limit: for water-bearing intervals with the content of highly-dispersed clay minerals of 40%, porosity exceeds 20%.

Electrical logs were used to estimate the intergranular porosity and initial oil saturation. Based on the log analysis, the oil saturation in fractures is about 100%, whereas the oil saturation in the matrix is about 50%. Weighted average oil saturation of the whole formation (including the secondary pores, vugs, and fractures) is about 90%.

Porosity and permeability were measured at a depth of 450 to 500 m from the top of volcanic rocks. Deeper intervals, i.e., from 1000 to 2000 m, are dry or showed insignificant flow of water. The most productive zone is the upper section of volcanic rocks, 25–30 m thick. Here, one can observe uniform and intensive secondary rock alterations and strong oil flow in most of the wells. The oil-saturated intervals are distributed from the top of volcanic rocks to a depth of 10–50 m in some wells, and to a depth of 100 m and deeper in others. As shown in Figure 1.20b, the bottom of oil accumulation is located at different depths in different volcanic rocks. This means that there is no continuous and flat oil-water contact; instead, it has a wave-shaped configuration. The real oil-reservoir boundaries intersect the contour lines on the top of volcanic rocks. Oil is present in the secondary porosity of these rocks.

The reservoirs are characterized by non-uniform oil content, both in lateral and vertical directions. Consequently, the initial oil production rates vary within the following wide limits:

1. 1 to 30 t/d (7 to 220 bbl/d) in 48% of wells.
2. 30 to 100 t/d (220 to 750 bbl/d) in 35% of wells.
3. >100 t/d (>750 bbl/d) in 17% of wells.

The maximum initial water production in most wells (58%) is 10 m^3/d. Initial reservoir pressure and temperature are 55 MPa and 125°C, respectively. The initial reservoir pressure is higher than the bubble-point pressure by 40 MPa and higher than the normal hydrostatic pressure by 20 MPa. Gas/oil ratio is equal to 30 m^3/t and the average density of oil is 0.880 g/cm^3 at standard conditions. The oil is paraffinic, with low sulfur content.

1.2.6 Classification of Hydrocarbon Accumulations Based on the Type of Traps

Hydrocarbon accumulations can be classified into three major types and subtypes (Eremenko and Chilingar, 1996):

I. *Traps formed by folding (with or without faults).* Accumulations formed as a result of folding are usually associated with the

bedded reservoirs. The complexity of structure (sometimes even isometric), size, and especially heights are caused by the trap and reservoir position in the sedimentary basin. Over the central areas of tectonic plates, the traps are gentle and sometimes very large. Over the plate margins, transition zones and, especially, collision zones, the folds are higher, steeper and with a clearly expressed trend. The accumulations may be classified using some other parameters, too. In particular, oil-water contours in such accumulations are closed and, in plan view, have oval or more intricate shapes, and form rings.

II. *Traps formed within various buildups.* Accumulations formed within various buildups are usually associated with the massive-type reservoirs. Most common are accumulations in biogenic buildups (reefs and bioherms). Sometimes, biostromes are mistakenly attributed to the same class. Included here are large accumulations with huge flow rates due to the presence of fractures and vugs in carbonates. Some investigators also include in this group the erosional projections of the metamorphic and volcanic rocks (fault-bounded or bounded by erosional surfaces), which may contain accumulations, e.g., White Tiger Field in Vietnam.

III. *Traps that are limited by the depositionally imposed facies changes.* Lithologic and stratigraphic traps of Group III include facies pinch-outs, stratigraphic unconformities, and contact of the reservoir with the impermeable rock up-section. Such traps may be associated with the bedded reservoirs on the monoclines or on the flanks of anticlines. These traps may contain rather large accumulations. They may be associated with bedded reservoirs confined on every side. In such a case, they form large accumulations. Water saturation contours impinge on the trap (impermeable barrier). This type of accumulations is very common: about 50% of all known accumulations.

Accumulations of Types I, II, and III are formed in accordance with the gravitational ("anticlinal") theory. By far, not all known accumulations, however, belong in the described three types or combinations thereof. Also, not all of them formed in accordance with the gravitational theory. These unconventional accumulations are discussed below (Types IV through VII).

IV. *Dominance of capillary forces over the gravity force.* Oil or gas found in hydrophilic rocks occupies coarser-grained

reservoir rocks, which are sealed by water-saturated fine-grained reservoir rocks. Examples of such accumulations associated with relatively coarse-grained sandstone lenses (e.g., 100-ft sandstone in Appalachian Oil and Gas Province, USA) were presented by Brod (1957). The authors of this book reviewed large number of commercial accumulations all over the world and have not been able to find another such clear-cut example. Although the appearance of capillary forces is frequently observed, the formation and preservation of the accumulations cannot be attributed to these forces. It should be kept in mind that water and gas lenses exist within oil accumulations; water is sometimes encountered updip in pinched-out reservoirs (e.g., Productive Series of the Absheron Peninsula in Azerbaijan, and Maykopian sandstones in the Northwestern Caucasus).

V. *Dominance of hydraulic forces.* The hydraulic forces (Figure 1.22) can cause a tilt in the oil- water interface. To determine that tilt, a trigonometric function or the Savchenko's (1977) equation could be used.

$$\Delta h = \Delta p_{norm} / g(\rho_{water} - \rho_{oil}) \tag{1.14}$$

where Δh is the amount of shift at the edge of accumulation, Δp_{norm} is the difference in normalized pressures; ρ_{water} and ρ_{oil} are the density of water and oil, respectively; and g is the gravitational acceleration.

A barrier (facies change, stratigraphic unconformity, and a fault) often turns out to be a barrier due to the presence of pressure difference across the barrier, rather than because of the appearance of an impermeable barrier in the way of fluid movement.

Figure 1.22 shows possible relations of the position of the piezometric surface (normalized pressure head) and the position of the oil-water contact. The necessary condition for the pore preservation of hydraulically-trapped accumulation next to a fault is a higher potential head of the water next to the fault zone than that of the productive formation (the surplus pressure is included). This condition may exist if, for instance, there is a communication along the fault between the accumulation and the reservoir with AHFP (overpressure).

In monoclines, the accumulations can be preserved (Figure 1.22c, e and f) if the potential head decreases down dip in locations where the dip increases (Figure 1.22e) or the dip of the piezometric surface

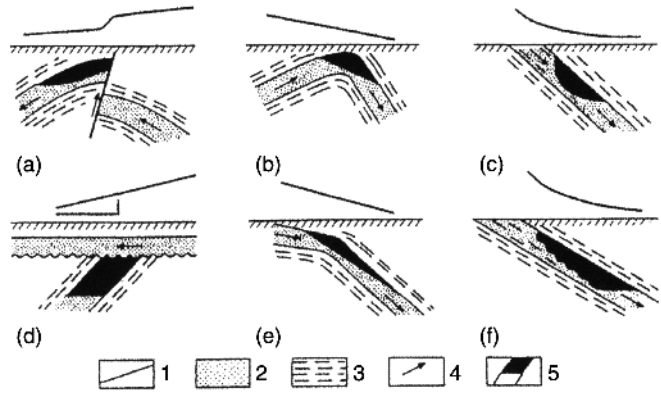

Figure 1.22 Conceptual cross-sections showing hydraulically trapped oil and gas accumulations. (a) Next to conductive faults. (b) At the anticlinal crest. (c) In monoclines within the areas of changing reservoir properties. (d) In monoclines underneath the stratigraphic unconformities. (e) At structural noses of monoclines. (f) Near the reservoir shale-out boundaries. 1 – Piezometric surface; 2 – reservoir; 3 – shales; 4 – direction of water movement; and 5 – oil and gas accumulations.

decreases (Figure 1.22f). The latter is possible when the reservoir-rock properties change (i.e., capillary forces enter into play). The oil-water contours can close onto themselves (but crossing the structural contour lines on top of the reservoir) or can abut on the trapping barrier. (The contributions of Plotnikov, 1976; Gattenberger, 1984; and Mikhaylov, 1984, on hydrodynamic traps are noteworthy.)

Neither of the described types, however, owes its existence to the hydraulic forces exclusively. They can exist only under condition of the combined interaction of several different forces: (1) hydraulic and gravity, (2) hydraulic and capillary, or (3) hydraulic + capillary + gravity forces. The effect of hydraulic forces is commensurate with that of gravity and capillary forces

VI. *Gas accumulations in synclines or in monoclines devoid of structural highs.* Examples of such accumulations have been presented by Masters (1979) and Perrodon (1984). There is a gas accumulation in the Deep Basin Monocline, in Alberta, Canada. The latter accumulation resides in the Mesozoic sandstone, which is more than 3 km high (the thickness of individual gas intervals is 10–150 m). The sandstone is water-saturated updip the gas accumulation, with an improvement in petrophysical properties. The gas reserves

are nearly 11.3 TCM. The gas accumulation of Milk River Field (Canada), with 250 BCM of reserves, is another similar example. The gas accumulation of San Juan Field (USA) resides in the Mesozoic sandstone in the synclinal part of the structure, with reserves of 700 BCM. The sandstone is water-saturated over the flanks. The porosity and permeability within the gas-saturated portion are 14% and 1 mD, respectively, whereas in the water-saturated portion, ϕ = 25% and k = 100 mD. For further discussion, see Chilingar *et al.* (2005).